NIH Consensus Development Conference (1992). Diagnosis and treatment of depression of late life. *JAMA*, 268, 1018–1029.

Penninx, B. W., Deeg, D. J., van Eijk, J. T., Beekman, A. T. and Guralnik, J. M. (2000). Changes in depression and physical decline in older adults: a longitudinal perspective. *Journal of Affective Disorders*, 61, 1–12.

Raveis, V. H., Karus, D. G. and Siegel, K. (1998). Correlates of depressive symptomatology among adult daughter caregivers of a parent with cancer. *Cancer*, 83, 1652–1663.

Schulz, R. *et al.* (2008). Dementia patient suffering and caregiver depression. *Alzheimer Disease and Associated Disorders*, 22, 170–176.

Sewitch, M. J., McCusker, J., Dendukuri, N. and Yaffe, M. J. (2004). Depression in frail elders: impact on family caregivers. *International Journal of Geriatric Psychiatry*, 19, 655–665.

Sherwood, P. R., Given, C. W., Given, B. A. and von Eye, A. (2005).Caregiver burden and depressive symptoms: analysis of common outcomes in caregivers of elderly patients. *Journal of Aging and Health*, 17, 125–147.

Soldato, M. *et al.* (2008). Patient depression and caregiver attitudes: results from The AgeD in HOme Care study. *Journal of Affective Disorders*, 106, 107–115.

Tsutsui, T. and Muramatsu, N. (2005). Care-needs certification in the long-term care insurance system of Japan. *Journal of the American Geriatrics Society*, 53, 522–527.

Wada, T. *et al.* (2004). Depression in Japanese community-dwelling elderly: prevalence and association with ADL and QOL. *Archives of Gerontology and Geriatrics*, 39, 15–23.

Yesavage, J. A. (1988). Geriatric Depression Scale. *Psychopharmacology Bulletin*, 24, 709–711.

Ca^{2+} channel blocker benidipine promotes coronary angiogenesis and reduces both left-ventricular diastolic stiffness and mortality in hypertensive rats

Takao Nishizawa[a], Xian Wu Cheng[a,f,g], Zhehu Jin[b,f], Koji Obata[c], Kohzo Nagata[d], Akihiro Hirashiki[a], Takeshi Sasaki[b], Akiko Noda[d], Kyosuke Takeshita[a], Hideo Izawa[a], Guo-Ping Shi[e], Masafumi Kuzuya[b], Kenji Okumura[a] and Toyoaki Murohara[a]

Background **The beneficial cardiac effects of some Ca^{2+} channel blockers have been attributed to blood pressure reduction, but these pleiotropic effects require further investigation. We compared the effects of benidipine, which has beneficial cardiac effects, and nitrendipine, which does not, in an animal model of hypertensive diastolic heart failure (DHF).**

Methods and results **Male Dahl salt-sensitive rats were fed a high-salt diet from age 7 weeks to induce hypertension and were either vehicle or orally administered benidipine (3 mg/kg daily) or nitrendipine (10 mg/kg daily) from age 10 to 18 weeks. Control rats were maintained on a low-salt diet. In vehicle-treated rats, left-ventricular (LV) fractional shortening was preserved but LV end-diastolic pressure was increased, indicative of DHF. Benidipine and nitrendipine had similar antihypertensive effects and reduced both LV weight and cardiomyocyte hypertrophy. Benidipine reduced LV diastolic stiffness and mortality to a greater extent than did nitrendipine. Benidipine, but not nitrendipine, also reduced lung weight. The extent of interstitial fibrosis and the abundance of mRNAs for prohypertrophic, profibrotic, or proinflammatory genes in the left ventricle were reduced by benidipine and nitrendipine. Benidipine, but not nitrendipine, increased capillary density and restored the expression of hypoxia-inducible factor 1α, vascular endothelial growth factor, and endothelial nitric oxide synthase in the left ventricle.**

Conclusions **Benidipine reduced LV diastolic stiffness and increased survival, effects likely attributable predominantly to promotion of coronary angiogenesis rather than to attenuation of interstitial fibrosis. Benidipine may thus be more effective than purely L-type Ca^{2+} channel blockers in preventing hypertensive DHF. *J Hypertens* 28:1515–1526 © 2010 Wolters Kluwer Health | Lippincott Williams & Wilkins.**

Journal of Hypertension 2010, 28:1515–1526

Keywords: angiogenesis, cardiac stiffness, diastolic heart failure, hypoxia-induced factor-α, L-type Ca^{2+} channel

Abbreviations: β-MHC, β-myosin heavy chain; ACE, angiotensin-converting enzyme; ACEI, angiotensin-converting enzyme inhibitor; ARB, angiotensin-receptor blocker; DHF, diastolic heart failure; DHP, dihydropyridine; eNOS, endothelial nitric oxide synthase; GAPDH, glyceraldehyde-3-phosphate dehydrogenase; HIF-1α, hypoxia-inducible factor-1α; IVST, interventricular septum; LV dP/dt_{max}, maximum first derivative of left ventricular pressure; LV dP/dt_{min}, minimal rate of left ventricular pressure; LVDd, left-ventricular end-diastolic dimension; LVDs, left-ventricular end-systolic dimension; LVH, left-ventricular hypertrophy; LV, left-ventricular; MR, mineralocorticoid receptor; PCR, polymerase chain reaction; $T_{1/2}$, the pressure half-time; TGF-1β, transforming growth factor-1β; VEGF, vascular endothelial growth factor

[a]Department of Cardiology, [b]Department of Geriatrics, Nagoya University Graduate School of Medicine, [c]Department of Pharmacology, Aichi Gakuin University School of Dentistry, [d]Department of Medical Technology, Nagoya University School of Health Sciences, Nagoya, Japan, [e]Department of Cardiovascular Medicine, Brigham and Women's Hospital, Harvard Medical School Boston, Massachusetts, USA, [f]Department of Cardiology, Yanbian University Hospital, Yanji, Jilin Province, China and [g]Department of Internal Medicine, Kyung Hee University Hospital, Seoul, Korea

Correspondence to Xian Wu Cheng, MD, PhD, Department of Cardiology, Nagoya University School of Medicine, 65 Tsuruma-cho, Nagoya 466-8550, Japan
Tel: +0081 52 744 2427; fax: +0081 52 744 2371;
e-mail: chengxw0908@yahoo.com.cn or xianwu@med.nagoya-u.ac.jp

Received 23 August 2009 **Revised** 13 February 2010
Accepted 16 March 2010

Introduction

Chronic pressure overload due to hypertension results in myocardial hypertrophy as an adaptive response to maintain cardiac function. However, persistent left-ventricular hypertrophy (LVH) leads to diastolic heart failure (DHF) [1,2], which accounts for 30–50% of all cases of heart failure and has a poor prognosis [3,4]. DHF is characterized by abnormal LV relaxation, impaired LV filling, and increased LV diastolic stiffness, with LV systolic function remaining largely unaffected.

Given that increased interstitial fibrosis has been associated with the onset of DHF [5], agents that block the renin–angiotensin–aldosterone system are used for the treatment of this condition [6]. However, given that treatment with a single antihypertensive angiotensin-converting enzyme inhibitor (ACEI) or angiotensin-receptor blocker (ARB) is often insufficient to normalize blood pressure, calcium channel blockers (CCBs) are often used in combination with ARBs or ACEIs in the clinical setting [7]. In addition to ACEI and ARB, recent

0263-6352 © 2010 Wolters Kluwer Health | Lippincott Williams & Wilkins

DOI:10.1097/HJH.0b013e328339fd3a

few studies in experimental animals have shown that CCBs are also effective in preventing cardiac remodeling and dysfunction [8]. In fact, it has been reported that CCBs exert cardiovascular protective actions including reduction of oxidative stress and proinflammatory response [2,9]. However, the precise mechanisms underlying the cardioprotection afforded by a CCB in animals or patients with hypertensive DHF remain largely unknown.

The physiological role of T-type Ca^{2+} channel is diverse, and clinical advantages of T-type channel blockade were assessed in late 1990s using mibefradil, another class Ca^{2+} channel antagonist. The drug had relatively selective blocking action on T-type Ca^{2+} channel, and beneficial effects were shown in the treatment of cardiac hypertrophy, angina pectoris and renal failure [10–12]. However, mibefradil, which is known to block all three subtypes of T-type Ca^{2+} channel (α_{1G}, α_{1H} and α_{1i}) [13], was abandoned for clinical usage because of frequent drug–drug interaction. In addition, some studies show that some dihydropyridines (DHPs) have blocking action T-type Ca^{2+} channels in native tissues [14,15]. As subtype-specific blocking action of DHPs was not assessed in these studies, different expression levels of each T-type channel subtype would result in different blocking action in case that DHP had subtype-specific blocking action.

Recent study has indicated that DHP Ca^{2+} antagonists have a different profile in blocking T-type Ca^{2+} channel subtypes expressed in *Xenopus* oocytes [16,17]. Several studies showed beneficial effect of efonidipine on renal function, cardiac failure and aldosterone secretion as a result of the T-type Ca^{2+} channel-blocking action of the drug [18–20]. Accumulating evidence suggested that up-regulation of T-type Ca^{2+} channels has been associated with both LVH and hypertensive DHF [21,22]. To elucidate the cardiac protective effects as well as the mechanism of action of benedipine against the activated T-type Ca^{2+} channel, we compared the effects of benidipine, a blocker of T-type and L-type Ca^{2+} channels, with those of nitrendipine, a blocker of L-type Ca^{2+} channel, in a Dahl salt-sensitive rat model of hypertensive DHF.

Methods

Animals

Male inbred Dahl salt-sensitive rats were obtained from Japan SLC (Hamamatsu, Japan) and were handled in accordance with the guidelines of Nagoya University Graduate School of Medicine as well as with the Guide for the Care and Use of Laboratory Animals (NIH publication no. 85–23, revised 1996). Weaning rats were fed laboratory chow containing 0.3% NaCl until 7 weeks of age. Animals on this latter diet served as models of hypertensive LVH at 10 weeks of age and DHF at 18 weeks of age [1]. Both food and tap water were provided *ad libitum* throughout the experiment. The rats on the high-salt diet were divided into three groups: those orally given benidipine (3 mg/kg body weight daily; Kyowa Hakko Kirin CO., Ltd, Tokyo, Japan) from 10 to 18 weeks of age ($n = 10$); those orally given nitrendipine (10 mg/kg daily; Sigma Aldrich) from 10 to 18 weeks of age ($n = 10$); and those orally given vehicle (0.5% carboxymethylcellulose) from 10 to 18 weeks of age ($n = 10$, untreated group). The benidipine, nitrendipine, and vehicle were each given by oral gavage every day. Rats maintained on the 0.3% NaCl diet until 18 weeks of age were studied as a control group ($n = 10$). At 18 weeks of age, rats were anesthetized by intraperitoneal injection of ketamine (50 mg/kg) and xylazine (10 mg/kg) and were subjected to hemodynamic and echocardiographic analyses. The heart and kidney were subsequently excised, and LV and kidney tissues were stored at −80°C for either molecular analyses, or fixed with paraformaldehyde for pathological analysis.

Echocardiographic and hemodynamic analyses

Systolic blood pressure was measured weekly in conscious animals by tail-cuff plethysmography (BP-98A; Softron, Tokyo, Japan) [23]. At 18 weeks of age, rats were subjected to transthoracic echocardiography as previously described [23]. Echocardiography was performed with a SONOS 7500 ultrasound system and an ultraband transducer of 5–12 MHz (Philips, Andover, Massachusetts, USA). LV end-diastolic (LVDd) and end-systolic (LVDs) dimensions as well as the thickness of the interventricular septum (IVST) were measured. LV fractional shortening was calculated as $100\% \times (\text{LVDd} - \text{LVDs})/\text{LVDd}$. After echocardiography, a 2F micromanometer-tipped catheter (SPR-407; Millar Instruments, Houston, Texas, USA) that had been calibrated relative to atmospheric pressure was inserted through the right carotid artery into the left ventricle. We evaluated the maximum first derivative of LV pressure (LV dP/dt_{max}) as an index of contractility, minimal rate of LV pressure change (LV dP/dt_{min}), and the pressure half-time ($T_{1/2}$) as an index of relaxation. Tracings of LV pressure and the electrocardiogram were digitized to determine the pressure half-time and LV end-diastolic pressure as previous described [2].

Histology

The left ventricle was fixed with ice-cold 4% paraformaldehyde for 16–24 h, embedded in paraffin, sectioned transversely (thickness 3 μm), and stained either with hematoxylin–eosin for evaluation of cardiomyocyte hypertrophy or with Azan-Mallory solution for evaluation of interstitial fibrosis. The cross-sectional areas of cardiomyocytes and the areas of the fibrosis in the interstitial region were calculated in 10 randomly chosen microscopic fields from three different sections in each animal, as previously described [24,25]. The sections of were also immunostained with mouse monoclonal antibody to rat CD31 (1:100 dilution; Pharmingen, San Diego,

California, USA), and a Universal Immuno-Enzyme Polymer kit (Nichirei Biosciences, Tokyo, Japan) was used to visualize the coronary capillary endothelial cells. The capillary endothelial cells were quantified by measuring the number of $CD31^+$ cells per high-power field (400×). The number of capillaries was measured in 15 randomly chosen microscopic fields from three different sections in each animal. The evaluation of capillary diameter was also analyzed in each high-power field (400×).

Quantitation of gene expression

Total RNA was extracted from LV tissue, and the abundance of specific mRNAs was determined by reverse transcription and real-time polymerase chain reaction (PCR) analysis with a Prism 7700 Sequence Detector (Perkin-Elmer, Waltham, Massachusetts, USA). The sequences of primers and TaqMan probes specific for β-myosin heavy chain (β-MHC), angiotensin-converting enzyme (ACE), transforming growth factor (TGF)-1β, or collagen types I or III have been described previously [25], as have been those for vascular endothelial growth factor (VEGF), VEGF receptor-1 (Flt-1), hypoxia-inducible factor (HIF)-1α, and endothelial nitric oxide synthase (eNOS) [24,25]. PCR was also performed with oligonucleotides specific for the α1G subunit of T-type Ca^{2+}channels (5′-CCTGCCTGTTGCCGA GAG-3′, 5′-CTGTCTGTGTTACTGGATTCCTTC C-3′, and 5′-AGATTCCTGGTCGGCCTATATCTT TCC-3′ as the forward primer, reverse primer, and TaqMan probe, respectively; GenBank accession no. AF027984). TaqMan rodent glyceraldehyde-3-phosphate dehydrogenase (GAPDH) control reagents (Applied Biosystems, Foster City, California, USA) were used to detect GAPDH mRNA as an internal standard.

Immunoblot analysis

Tissue samples (80 μg of protein) were subjected to sodium dodecyl sulfate-polyacrylamide gel electrophoresis on a 10% gel, and the separated proteins were transferred to a polyvinylidene difluoride membrane (Bio-Rad Laboratories, Hercules, California, USA). The membrane was incubated at room temperature, first for 1 h with Tris-buffered saline containing 5% nonfat milk and 0.1% Tween-20 and then overnight with rabbit polyclonal antibodies to VEGF-A, to VEGF-C (Santa Cruz Biotechnology, Inc., Santa Cruz, California, USA), to HIF-1α (Novus Biologicals, Littleton, Colorado, USA), to Phosepho-eNOs (p-eNOs, Ser-1177), or to eNOS (both from Cell Signaling, Danvers, Massachusetts, USA), all at a 1 : 1000 dilution in the same solution. The membrane was washed and then incubated at room temperature for 1 h with a 1 : 1000 dilution of horseradish peroxidase-conjugated goat antibodies to rabbit immunoglobulin G (MBL, Nagoya, Japan), after which immune complexes were detected and quantified as described previously [24]. The intensities of the VEGF, HIF-1α, and eNOS bands were quantified by densitometry with ATTO CS Analyzer (version 1.01) software, and the amount of each protein was normalized against that of GAPDH determined with rabbit antibodies to this protein (Santa Cruz Biotechnology, Inc.).

Statistics

Data are presented as means ± SEM. Differences in various parameters between the four groups were evaluated by analysis of variance (ANOVA) followed by Dunnett's post-hoc test. Survival rate was analyzed by the standard Kaplan–Meier method with a log-rank test. A P value of less than 0.05 was considered statistically significant.

Statement of responsibility

The authors had full access to the data and take responsibility for data integrity. All authors have read and agree to the manuscript as written.

Results

Systolic blood pressure

Dahl salt-sensitive rats fed a high-salt diet from 7 weeks of age progressively developed hypertension [1,2]. Treatment with benidipine or nitrendipine from 10 weeks of age similarly lowered systolic blood pressure by approximately 15–20 mmHg in the conscious state, with this effect being apparent as early as 1 week after the initiation of treatment (Fig. 1, Table 1).

Survival rate

Kaplan–Meier analysis revealed that the survival rate of rats in the untreated group up to 18 weeks of age was half that of animals in the control group (no deaths). The survival rate was increased slightly in the nitrendipine

Fig. 1

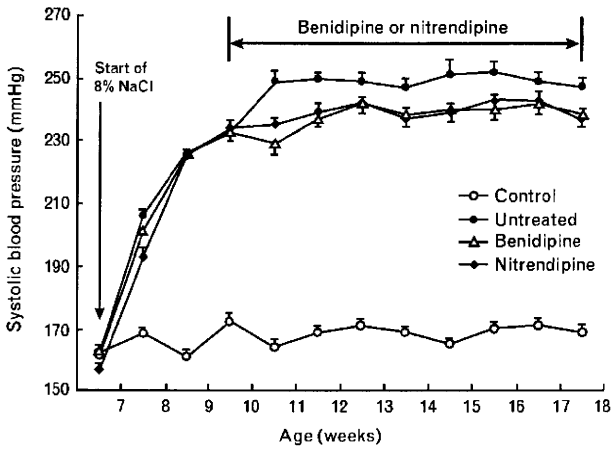

Time course of systolic blood pressure in Dahl salt-sensitive rats fed a high-salt diet from 7 weeks of age and treated with vehicle (untreated group), benidipine (3 mg/kg daily), or nitrendipine (10 mg/kg daily) from 10 weeks of age, as well as in age-matched controls fed a low-salt diet (control group). Data are means ± SEM (n = 10 per group).

Table 1 Hemodynamic, echocardiographic, and pathological parameters in Dahl salt-sensitive rats of the four experimental groups at 18 weeks of age

Parameter	Control	Untreated	Benidipine	Nitrendipine
SBP (mmHg)	172 ± 3	253 ± 5*	234 ± 9*,**	235 ± 7*,**
Heart rate (b.p.m.)	466 ± 18	524 ± 12	450 ± 13**,***	511 ± 7
IVST (mm)	1.91 ± 0.05	2.50 ± 0.12*	2.10 ± 0.06*,**	2.20 ± 0.08*,**
LVDd (mm)	8.07 ± 0.16	7.81 ± 0.11	7.97 ± 0.33	8.00 ± 0.40
LVFS (%)	44.7 ± 1.5	42.5 ± 3.6	44.0 ± 2.8	44.2 ± 3.8
LV dP/dt_{max} (mmHg/s)	8271 ± 260	7890 ± 156*	10234 ± 347*,**	10877 ± 932*,**
LV dP/dt_{min} (mmHg/s)	7654 ± 324	7022 ± 108*	7634 ± 434**	8023 ± 663**
$T_{1/2}$ (ms)	3.8 ± 0.2	6.2 ± 0.3*	4.9 ± 0.3*,**	5.1 ± 0.3*,**
LVEDP (mmHg)	3.9 ± 0.2	11.7 ± 0.2*	3.8 ± 0.4**,***	8.1 ± 0.3*,**
LV weight (mg)/BW (g)	2.11 ± 0.02	4.20 ± 0.12*	2.94 ± 0.07*,**	3.05 ± 0.16*,**
Lung weight (mg)/BW (g)	2.76 ± 0.07	8.01 ± 1.01*	3.51 ± 0.12*,**,***	6.11 ± 1.06*,**

SBP, systolic blood pressure; IVST, interventricular septum thickness; LVDd, left-ventricular end-diastolic dimension; LVFS, left-ventricular fractional shortening; LV dP/dt_{max} and LV dP/dt_{min}, first derivative of maximum or minimum left ventricular pressure, respectively, with respect to time; $T_{1/2}$, time constant of LV pressure decay; LVEDP, left-ventricular end-diastolic pressure; LV weight, weight of the left ventricle; BW, body weight. Data are means ± SEM ($n = 5$ per group). * $P < 0.05$ versus control group. ** $P < 0.05$ versus untreated group. *** $P < 0.05$ versus nitrendipine group.

group (60%) compared with that in the untreated group (50%), but no deaths were observed in the benidipine group (Fig. 2).

Left-ventricular geometry and function

Heart rate was greater in the untreated group than in the control group at 18 weeks of age, although this increase was not significant. Heart rate was significantly reduced by treatment with benidipine compared with that in the untreated and nitrendipine groups (Table 1). Both the thickness of the IVST and the ratio of LV weight to body weight were significantly greater in the untreated group than in the controls, indicative of LVH; both of these effects were significantly reduced by nitrendipine or benidipine. LV fractional shortening did not differ among the four experimental groups. The LV dP/dt_{max} was lower in the untreated group than in the control group; this change was improved by benidipine and nitrendipine. The LV dP/dt was smaller, whereas the $T_{1/2}$ was greater in the untreated group than in the controls. The changes in these parameters were also improved by both treatments.

Fig. 2

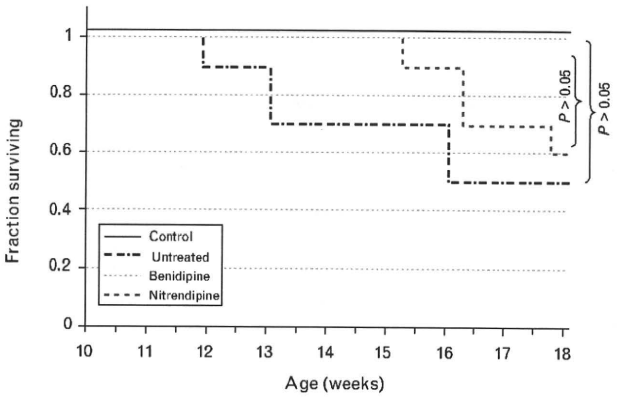

Kaplan–Meier plots of survival rates of Dahl salt-sensitive rats in the four experimental groups ($n = 10$ per group).

The LV end-diastolic pressure and the ratio of lung weight to body weight were greater in the untreated group than in the control group. Nitrendipine significantly reduced the extent of both parameters, whereas benidipine prevented it. In addition, the weight of the right-ventricular free wall was slightly increased in the untreated rats (0.21 ± 0.04 versus 0.19 ± 0.01 g in the controls; $P > 0.05$); this change was not improved by either treatment (0.22 ± 0.04 g with nitrendipine and 0.20 ± 0.03 g with benidipine; $P > 0.05$). Given that the LVDd assessed by echocardiography did not differ among the four experimental groups (Table 1), LV diastolic stiffness (LV end-diastolic pressure/LVDd) was significantly greater in the untreated group than in the controls (Fig. 3). Nitrendipine reduced this increase in stiffness to a level significantly lower than in the untreated group but still significantly higher than in the controls, whereas benedipine prevented it completely (Fig. 3).

Cardiomyocyte hypertrophy and interstitial fibrosis

Both the cardiomyocyte cross-sectional area (Fig. 4) and the level of interstitial fibrosis (Fig. 5) in the left ventricle were significantly greater in untreated rats than in control animals at 18 weeks of age. Benidipine or nitrendipine reduced the extents of both cardiomyocyte hypertrophy and interstitial fibrosis, but these parameters still remained significantly higher than the control values.

Coronary capillary density and diameter

Immunostaning revealed that the ratio of the number of coronary capillaries to that of cardiomyocytes was significantly greater in the untreated than in the control group; the ratio in the benedipine group was significantly greater than in the untreated and nitrendipine groups (Fig. 6a, b). Capillary density, however, was significantly lower in the untreated group than in the control group as a result of the cardiomyocyte hypertrophy evident in untreated animals (Figs 4a and 6c). Benidipine restored capillary density to the level in the control group, despite the residual

Fig. 3

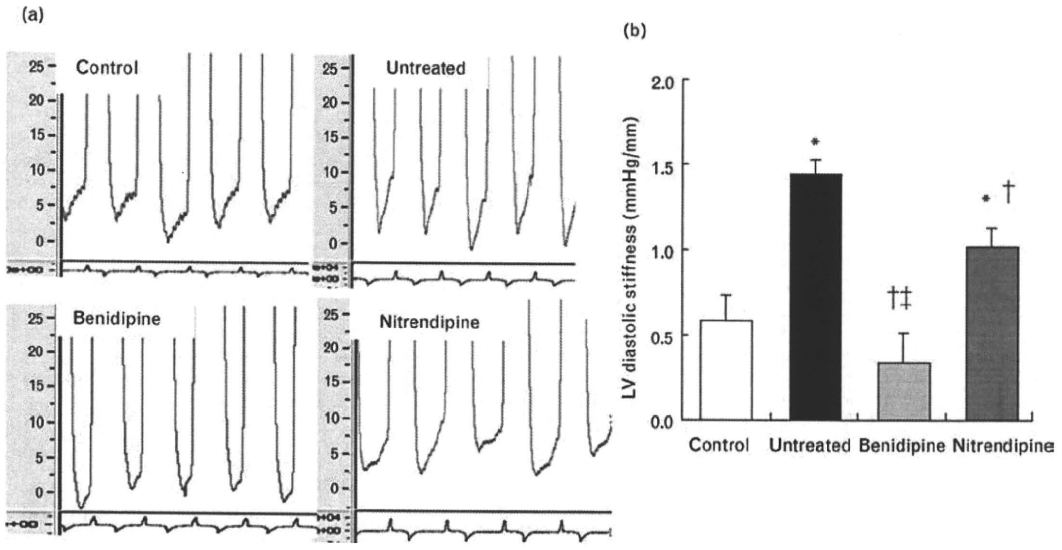

Left-ventricular (LV) pressure recordings and LV diastolic stiffness values in Dahl salt-sensitive rats of the four experimental groups at 18 weeks of age. (a) Representative waveforms obtained from a pressure manometer inserted into the left ventricle. (b) LV diastolic stiffness (LV end-diastolic pressure/LV end-diastolic dimension). Data are means ± SEM ($n = 5$ per group). $^{*}P < 0.05$ versus control group; $^{\dagger}P < 0.05$ versus untreated group; $^{\ddagger}P < 0.05$ versus nitrendipine group.

cardiomyocyte hypertrophy in benidipine-treated rats. As indicated in the representative sections stained for CD31 (Fig. 6a), more coronary capillaries appeared to be dilated in untreated or nitrendipine-treated rats than in control or benidipine-treated animals. Indeed, quantitative analysis revealed that the diameter of coronary capillaries was significantly smaller in benidipine-treated rats than in animals of the other three experimental groups (Fig. 6d).

Fig. 4

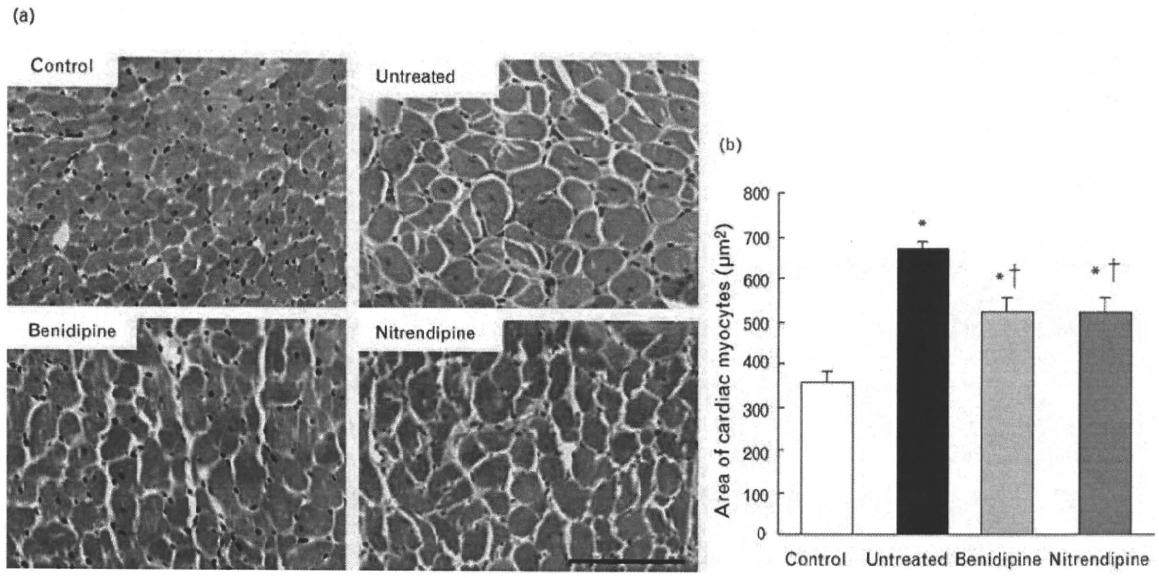

Cardiomyocyte hypertrophy in Dahl salt-sensitive rats of the four experimental groups at 18 weeks of age. (a) Representative hematoxylin–eosin staining of sections of the left ventricle. Scale bar, 100 μm. (b) Cross-sectional cardiomyocyte area, as measured in 10 randomly chosen microscopic fields from three different sections in each tissue block, similar to those shown in (a). Data are means ± SEM ($n = 5$ per group). $^{*}P < 0.05$ versus control group; $^{\dagger}P < 0.05$ versus untreated group.

Fig. 5

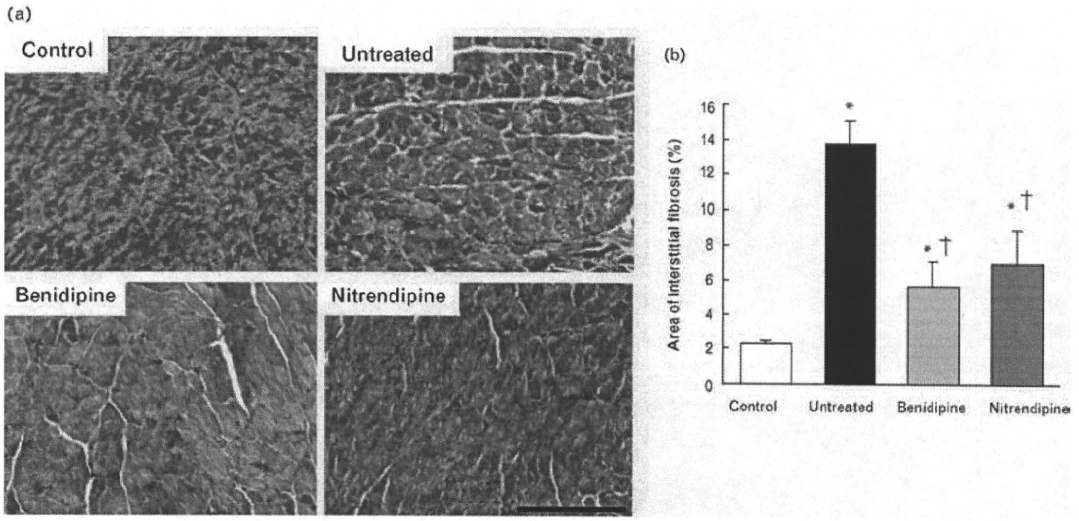

Interstitial fibrosis in the left ventricle of Dahl salt-sensitive rats in the four experimental groups at 18 weeks of age. (a) Representative Azan-Mallory staining of sections of the left ventricle. Scale bar, 200 μm. (b) Percentage area of interstitial fibrosis measured in 10 randomly chosen microscopic fields from three different sections in each tissue block, similar to those shown in (a). Data are means ± SEM ($n = 5$ per group). $^{*}P < 0.05$ versus control group; $^{\dagger}P < 0.05$ versus untreated group.

Gene expression

Hemodynamic overload resulted in up-regulation of the expression of the genes encoding β-MHC, ACE, TGF-β1, and collagen types I and III in the left ventricles of untreated rats at 18 weeks of age (Table 2). It also increased the ratio of the amount of collagen type I mRNA to that of collagen type III mRNA, an indicator of LV stiffness [23,25]. These increases in gene expression, with the exception of the increase in collagen type III mRNA abundance, were partly inhibited by treatment with benidipine or nitrendipine. Expression of the gene encoding the α1G subunit of T-type Ca^{2+} channels was also significantly higher in the untreated group than in the controls; this increase was reduced to a greater extent by treatment with benidipine than by that with nitrendipine (Table 2). The levels of VEGF, HIF-1α, eNOS, and Flt-1 mRNAs were significantly lower in the left ventricles of untreated-group rats than in the control-group rats; these changes were improved by treatment with benidipine but not with nitrendipine (Figs 7a–c and 8b). Similarly, benidipine, but not nitrendipine, significantly increased the levels of VEGF, HIF-1α, and p-eNOS proteins compared with those in the untreated group (Fig. 7d–f). However, there were no differences in the levels of eNOS protein among the four experimental groups (Fig. 8a).

Renal fibrosis

Histological analysis showed that the level of interstitial fibrosis was significantly greater in the kidneys of untreated rats than in control animals at 18 weeks of age; this change was improved by benidipine or nitrendipine, but these parameters remained significantly higher than the control values (Fig. 8c and d). The level of serum creatinine was higher in untreated rats than in control rats (0.41 ± 0.04 versus 0.28 ± 0.3 mg/dl, respectively; $P < 0.05$); this change was not improved by either treatments (0.41 ± 0.10 mg/dl with benidipine and 0.45 ± 0.09 mg/dl with nitrendipine; $P > 0.05$).

Discussion

We showed that benidipine, but not nitrendipine, promoted coronary angiogenesis, likely accounting for the reduction in both LV diastolic stiffness and death rate induced by treatment with this drug in our animal model of hypertensive DHF.

Effects of benidipine on diastolic dysfunction and mortality

We inspected the general condition of Dahl salt-sensitive rats in each experimental group every day, and we found that high-salt diet rats developed rapid and labored respiration. All animals that died were immediately subjected to postmortem examination, including macroscopic inspection of the intracranial, thoracic, and abdominal cavities. Cerebral hemorrhage or infarction, aortic rupture, or colonic ischemia was not detected, but all animals that died before 18 weeks of age manifested marked pulmonary congestion (as evidenced by an increase in the ratio of lung weight to body weight), indicating that congestive heart failure – not stroke – was the major cause of death.

Fig. 6

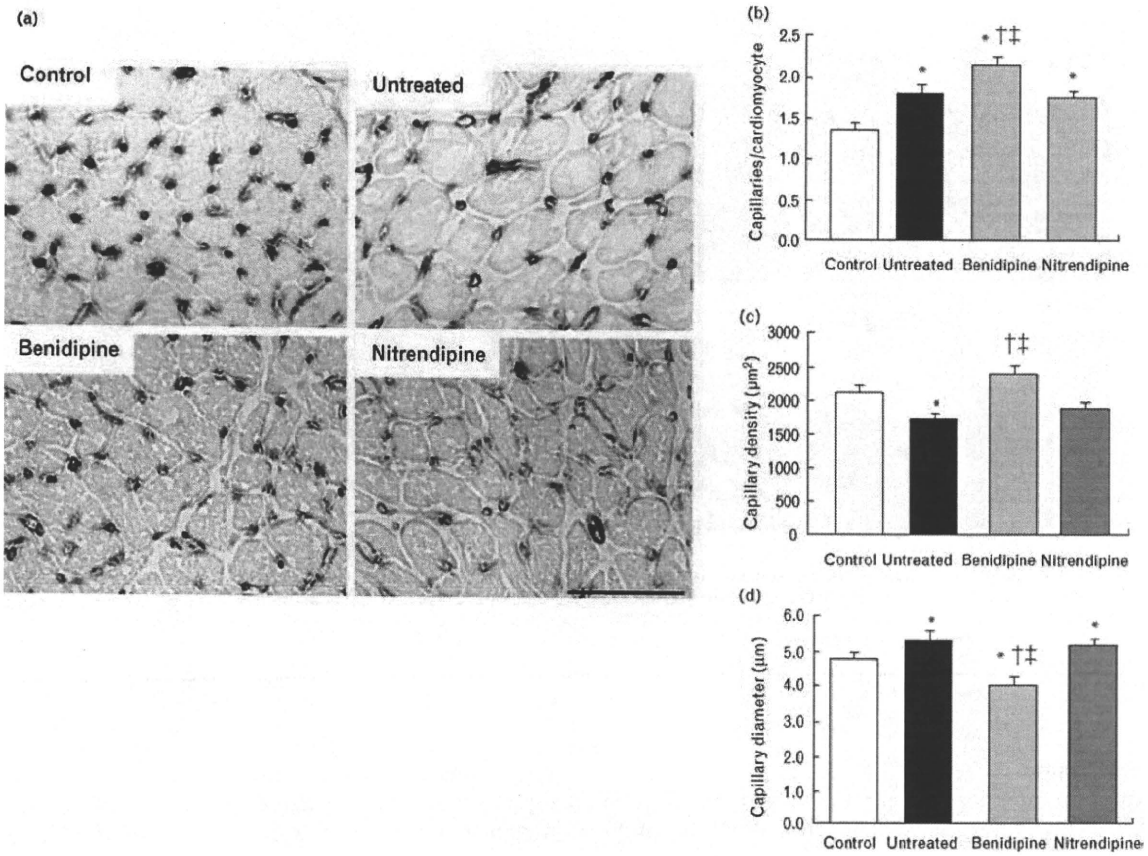

Coronary capillaries in the left ventricle of Dahl salt-sensitive rats in the four experimental groups at 18 weeks of age. (a) Representative CD31 immunostaining of sections of the left ventricle. Scale bar, 100 μm. (b–d) Ratio of the number of coronary capillaries to that of cardiomyocytes (b); capillary density (c); and capillary diameter (d) were measured in 15 randomly chosen microscopic fields from three different sections in each tissue block, similar to those shown in (a). The number of capillaries was measured in 15 randomly chosen microscopic fields from three different sections in each tissue block. Quantitative data are means ± SEM ($n = 5$ per group). $^{*}P < 0.05$ versus control group; $^{\dagger}P < 0.05$ versus untreated group; $^{\ddagger}P < 0.05$ versus nitrendipine group.

The diastolic dysfunction that develops in this animal model has been well characterized [5]. The time constant of LV pressure decay increases in association with the development of compensatory LVH. This time constant does not increase further with the development of DHF, which is accompanied instead by an increase in LV end-diastolic pressure. The relaxation delay is thus not likely to be a major contributor to the increase in end-diastolic pressure [26]. Our untreated group exhibited significant increases in both the time constant of LV pressure decay and LV end-diastolic pressure. Although benidipine and nitrendipine improved relaxation properties to similar

Table 2 Expression of prohypertrophic, profibrotic, or proinflammatory genes in the left ventricles of Dahl salt-sensitive rats in the four experimental groups at 18 weeks of age

Gene	Control	Untreated	Benidipine	Nitrendipine
β-MHC	1.0 ± 0.2	3.7 ± 0.7*	1.9 ± 0.2*,**	1.9 ± 0.2*,**
TGF-β1	1.0 ± 0.1	2.0 ± 0.3*	1.2 ± 0.1**	1.2 ± 0.2**
ACE	1.0 ± 0.2	1.7 ± 0.1*	1.1 ± 0.1**	1.0 ± 0.1**
Collagen type I	1.0 ± 0.2	4.0 ± 0.7*	2.6 ± 0.4*,**	2.5 ± 0.3*,**
Collagen type III	1.0 ± 0.2	3.0 ± 0.5*	2.6 ± 0.3*	2.5 ± 0.2*
Collagen type I/III ratio	1.0 ± 0.1	1.4 ± 0.2*	1.1 ± 0.1**	1.1 ± 0.1**
TCC α1G	1.0 ± 0.1	3.2 ± 0.6*	1.2 ± 0.2*,**,***	2.4 ± 0.3*,**

The amount of each mRNA in the left ventricle was determined by RT and real-time PCR analysis, normalized by that of GAPDH mRNA, and expressed relative to the normalized value for the control group. TCC α1G, α1G subunit of T-type Ca^{2+} channels. Data are means ± SEM ($n = 5$ per group). $^{*}P < 0.05$ versus control group. $^{**}P < 0.05$ versus untreated group. $^{***}P < 0.05$ versus nitrendipine group.

Fig. 7

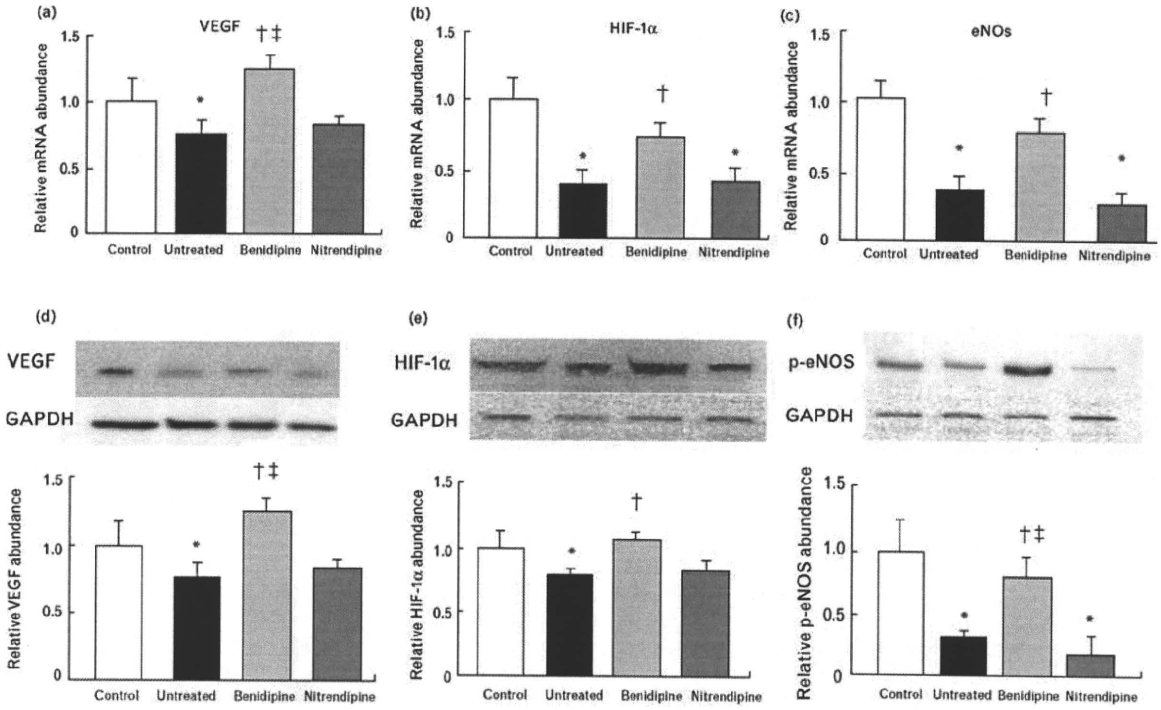

Expression of VEGF, HIF-1, and eNOS in the left ventricle of Dahl salt-sensitive rats in the four experimental groups at 18 weeks of age. (a–c) Abundances of VEGF, HIF-1, and eNOS mRNAs, respectively, as determined by RT and real-time PCR analysis. Data were normalized by the amount of GAPDH mRNA and then expressed relative to the normalized value for the control group; they are means ± SEM ($n = 5$ per group). (d–f) Abundances of VEGF, HIF-1, and eNOS proteins, respectively, as determined by immunoblot analysis. Representative blots are shown in the upper panels, and quantitative data (means ± SEM) are presented in the lower panels. The amount of each protein was normalized by that of GAPDH and then expressed relative to the normalized value for the control group. $^{*}P < 0.05$ versus control group; $^{\dagger}P < 0.05$ versus untreated group; $^{\ddagger}P < 0.05$ versus nitrendipine group ($n = 5$ per group). eNOS, endothelial nitric oxide synthase; GADPH, glyceraldehyde-3-phosphate dehydrogenase; HIF-1, hypoxia-inducible factor-1; VEGF, vascular endothelial growth factor.

extents, benidipine induced a greater reduction in the acute pressure increase from the end of relaxation to late diastole (Fig. 3a), resulting in prevention of DHF and improved survival.

Effect of benidipine on left-ventricular diastolic stiffness

Excess interstitial fibrosis or collagen deposition is associated with increased diastolic stiffness and pulmonary edema or congestive heart failure [27,28]. Among various mechanisms that contribute to LV diastolic stiffness [26], abnormalities in the transcriptional or post-transcriptional regulation of collagen genes result in the disproportionate accumulation of fibrous tissue during the development of LVH. Increased LV diastolic stiffness during the development of DHF has been associated with increased interstitial fibrosis in hypertensive Dahl salt-sensitive rats [2,5]. However, although we found that benidipine reduced LV diastolic stiffness to a greater extent than did nitrendipine, the inhibitory effects of the two drugs on both interstitial fibrosis and the expression of profibrotic genes were similar. These results thus suggested that the superior effect of benidipine on LV diastolic stiffness was attributable to an action other than inhibition of interstitial fibrosis.

Effect of benidipine on coronary angiogenesis

In this study, we observed that the capillary-to-cardiomyocyte ratio was increased by 14%, and the capillary density was decreased by 18%, in the left ventricles of Dahl salt-sensitive rats in the untreated group, compared with the corresponding values in control animals. Benidipine induced a further increase in the capillary-to-cardiomyocyte ratio (40% increase compared with the control group), resulting in complete restoration of capillary density; nitrendipine had no such effects. Coronary capillaries were significantly smaller in the benidipine group than in the other three groups; most of the capillaries in the untreated and nitrendipine groups appeared dilated. These observations suggest that the decreased capillary ratio and density present in the untreated and nitrendipine groups may dilate fully to maximize blood flow, whereas the coronary reserve is sufficient in the benidipine group. Alternatively, the large capillaries observed in the untreated and nitrendipine groups may

Fig. 8

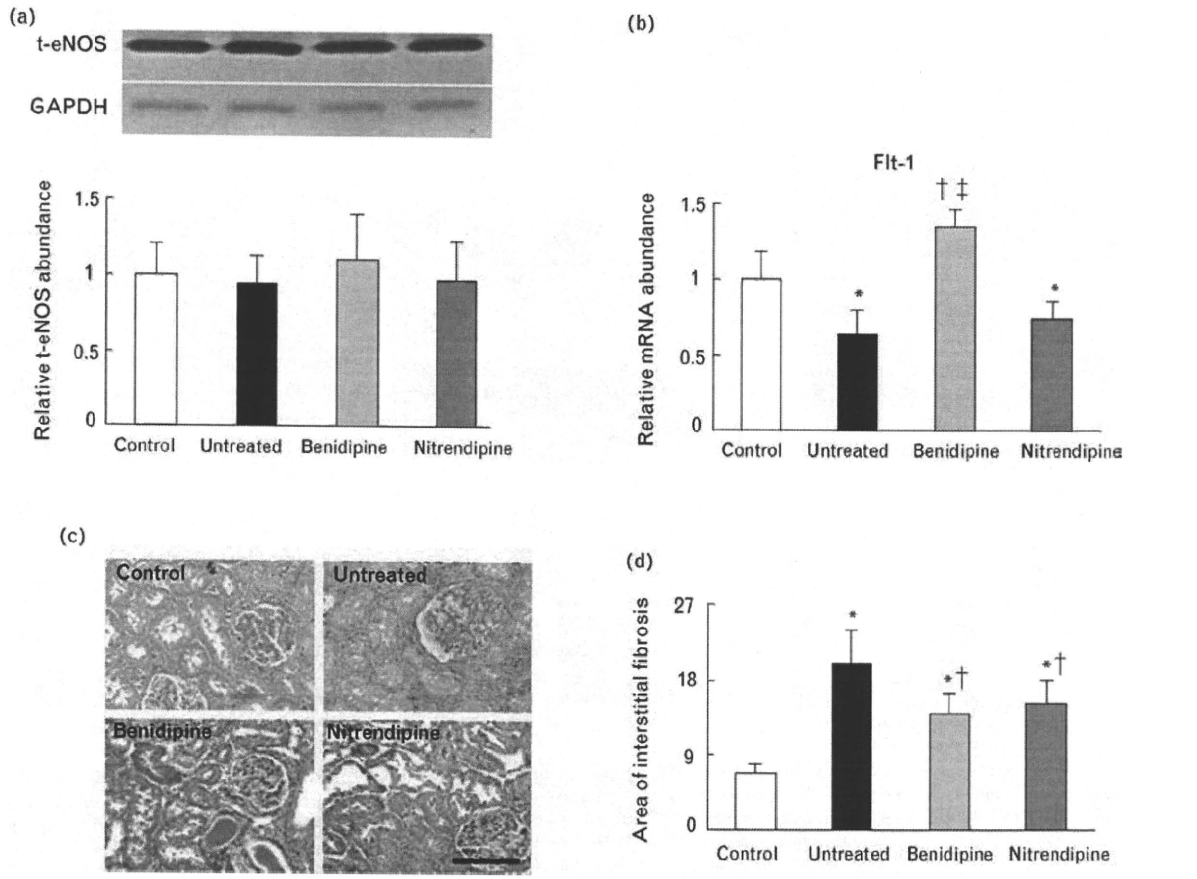

Levels of total eNOS (t-eNOS) protein, Flt-1 mRNA, and renal interstitial fibrosis in the four experimental groups at 18 weeks of age. (a) Abundance of t-eNOS protein, as determined by immunoblot analysis. (b) Abundance of Flt-1 mRNA, as determined by real-time PCR analysis. (c) Representative Azan-Mallory stainings of sections of the left ventricle. Scale bar, 100 μm. (d) Percentage area of interstitial fibrosis measured in 10 randomly chosen microscopic fields from three different sections in each tissue block, similar to those shown in (c). Data are means ± SEM ($n = 5$ per group). $^{*}P < 0.05$ versus control group; $^{\dagger}P < 0.05$ versus untreated group; $^{\ddagger}P < 0.05$ versus nitrendipine group. eNOS, endothelial nitric oxide synthase.

be mature, whereas the small vessels in the benidipine group may be newly generated. Given that angiogenesis results in degradation of surrounding interstitial fibrosis, benidipine might have been expected to reduce interstitial fibrosis to a greater extent that did nitrendipine; however, the two drugs had similar effects on cardiac fibrosis.

Effects of benidipine on vascular endothelial growth factor, hypoxia-inducible factor-1α, and endothelial nitric oxide synthase expression

Cardiomyocyte hypertrophy is thought to increase diffusion distance, contributing to a reduction in oxygen supply to the myocardium. Neovascularization associated with cardiac hypertrophy may be attributable to up-regulation of the expression of angiogenic factors in cardiomyocytes. HIF-1α is a transcription factor that induces expression of the VEGF gene in response to hypoxia–ischemia [29]. Angiogenesis in the vicinity of hypertrophic cardiomyocytes played an important role in preventing the transition from cardiac hypertrophy to LV systolic dysfunction in a mouse model of LVH [30]. In our model, coronary angiogenesis associated with cardiomyocyte hypertrophy was also implicated in preventing the transition from cardiac hypertrophy to DHF. When cardiac hypertrophy reaches a certain extent, even if ischemia persists, HIF-1α synthesis is down-regulated, with the result that the production of VEGF and angiogenesis also cease [30]. The VEGF-induced activation of protein kinase AKT and consequent phosphorylation of eNOS play a central role in angiogenesis [31,32]. Up-regulation of eNOS has also been found to modify angiogenesis in ischemic tissues [33]. It has previously been reported that the drug had relatively selective blocking action on T-type Ca^{2+} channel, and favorable actions were shown in cardiovascular system [10,19]. Here, we have

demonstrated that benidipine (but not nitrendipine) increased the levels of HIF-1α, VEGF, and eNOS mRNAs and proteins in the LV tissues of DHF rats. Taken together, these findings suggested that the blockade of cardiac T-type Ca^{2+} channel promotes ischemia-induced angiogenic response by enhancing HIF-1α-mediated VEGF and eNOS expressions in the myocardium of DHF rats. It should be noted that there was a discrepancy in cardiac T-type Ca^{2+} channel blockade-mediated angiogenic action associated with HIF-1α/eNOS/VEGF signaling pathway activation and morphological and functional improvement with the two drug interventions. Dihydropyridine nitrendipine has been shown to inhibit mineralocorticoid receptor activation *in vitro* and/or *in vivo* [34]. Recent studies have demonstrated that mineralocorticoid receptor blockade by antagonists results in attenuation of LV hypertrophy and heart failure in humans and in the Dahl salt-sensitive rat model [35,36]. Taken together, these findings suggest that the nitrendipine-mediated improvements in LV hypertrophy, fibrosis, and function are not attributable to the angiogenic action-linked HIF-1α/eNOS/VEGF signaling pathway activation by T-type Ca^{2+} channel blockade, but rather to the inhibition of mineralocorticoid receptor activation.

Relationship between cardiomyocyte hypertrophy-associated angiogenesis and left-ventricular diastolic stiffness

A mismatch between the number of capillaries and the size of cardiomyocytes, resulting in myocardial hypoxia, is thought to arise during the development of cardiac hypertrophy [37,38]. A relationship between cardiac angiogenesis, cardiac hypertrophy, and cardiac systolic function is also thought to exist [39–41]. With regard to diastolic function, the hypertrophic myocardium appears especially susceptible to nitric oxide donors; this resulted in a marked reduction in LV end-diastolic pressure in one clinical study [42]. Our present results suggest that benidipine reduces diastolic stiffness and prevents the transition from compensatory LVH to DHF, not only by inhibiting the development of interstitial fibrosis but also by promoting coronary angiogenesis. Improved blood flow and function are associated with evidence of angiogenesis in an ischemic region of heart [43]. Because benidipine promoted coronary angiogenesis and improved LV diastolic stiffness, it is plausible that benidipine increases myocardial blood flow and myocardial function in a genomic and/or nongenomic way. Hypoxia increases isovolumic resting tension in the isolated guinea pig heart [44] and raises the diastolic PV curve in humans during balloon coronary angioplasty [45]. Further studies to clarify the influence of ischemia on cardiomyocyte resting tension or cardiomyocyte distensibility in hypertensive DHF are warranted.

Study limitations

Up-regulation of T-type Ca^{2+} channels has been associated with both hypertensive LVH [21] and DHF [12]. We compared the effects of benidipine, a blocker of T-type and L-type Ca^{2+} channels, with those of nitrendipine, a blocker of L-type Ca^{2+} channel [22], in a rat model of hypertensive DHF. Inhibition of T-type Ca^{2+} channels by benidipine may underlie the promotion of angiogenesis by this drug. Current through these channels and expression of their α1G subunit are increased in association with the development of LVH [12,37]. Here, we could not measure T-type Ca^{2+} channel current in isolated cardiomyocytes from rats in the four experimental groups. Whereas benidipine and nitrendipine each inhibited the progression of LVH to similar extents, benidipine inhibited the increase in abundance of the α1G subunit mRNA apparent in the left ventricle of untreated Dahl salt-sensitive rats to a greater extent than did nitrendipine, suggesting that current through these channels was reduced by benidipine treatment. Further studies are warranted to clarify the relationship between inhibition of T-type Ca^{2+} channel current and coronary angiogenesis during the development of DHF. In addition, it is better to calculate peak flow velocities at the mitral level during rapid filling (*E*) and during atrial contraction (*A*), as well as the *E/A* ratio, the deceleration time, and the isovolumic relaxation time, from the pulsed Doppler echocardiographic data for assessment of LV diastolic function. Our study did not include an evaluation of these cardiac diastolic function indices.

Clinical implications

We have demonstrated that benidipine reduced LV diastolic stiffness and increased survival in hypertensive Dahl salt-sensitive rats to a greater extent than did nitrendipine. The prevention of DHF by benidipine appeared to be due predominantly to the promotion of angiogenesis rather than to inhibition of interstitial fibrosis, and this effect on angiogenesis appeared to be mediated by up-regulation of the production of HIF-1α, VEGF, and eNOS. Benidipine may thus be more effective than purely L-type Ca^{2+} channel blockers in preventing hypertensive DHF. Given that ARBs and ACEIs are widely used and are more effective than CCBs for the treatment of LVH, the latter drugs are considered to be potential second-line agents in combination therapy. The effects of combinations of ARBs or ACEIs with different types of CCBs, including a blocker of T-type and L-type Ca^{2+} channels benidipine, thus warrant testing in clinical trials.

Acknowledgements

We appreciate the technical assistance of A. Inoue, M. Miyachi and M. Kato.

The work was supported in part by grants from the Ministry of Education, Culture, Sports, Science, and Technology of Japan (nos. 17590719 and 19590812 to X.W.C.) and from the Japan Heart Foundation (no. 26-7508 to X.W.C.); by a Japan Heart Foundation/Novartis

Research Award on Molecular and Cellular Cardiology (no. 26-7523 to X.W.C); and by a grant from the Takeda Science Foundation (no. 26-7527 to X.W.C).

The authors declare no conflict of interest with regard to the present study. Benedipine was donated by Kyowa Hakko Kirin Co., Ltd. (Tokyo, Japan).

References

1 Doi R, Masuyama T, Yamamoto K, Doi Y, Mano T, Sakata Y, *et al.* Development of different phenotypes of hypertensive heart failure: systolic versus diastolic failure in Dahl salt-sensitive rats. *J Hypertens* 2000; **18**:111–120.

2 Cheng XW, Okumura K, Kuzuya M, Jin Z, Nagata K, Obata K, *et al.* Mechanism of diastolic stiffening of the failing myocardium and its prevention by angiotensin receptor and calcium channel blockers. *J Cardiovasc Pharmacol* 2009; **54**:47–56.

3 Vasan RS, Larson MG, Benjamin EJ, Evans JC, Reiss CK, Levy D. Congestive heart failure in subjects with normal versus reduced left ventricular ejection fraction: prevalence and mortality in a population-based cohort. *J Am Coll Cardiol* 1999; **33**:1948–1955.

4 Senni M, Tribouilloy CM, Rodeheffer RJ, Jacobsen SJ, Evans JM, Bailey KR, Redfield MM. Congestive heart failure in the community: a study of all incident cases in Olmsted County, Minnesota, in 1991. *Circulation* 1998; **98**:2282–2289.

5 Masuyama T, Yamamoto K, Sakata Y, Doi R, Nishikawa N, Kondo H, *et al.* Evolving changes in Doppler mitral flow velocity pattern in rats with hypertensive hypertrophy. *J Am Coll Cardiol* 2000; **36**:2333–2338.

6 Angeja BG, Grossman W. Evaluation and management of diastolic heart failure. *Circulation* 2003; **107**:659–663.

7 Chrysant SG, Bakris GL. Amlodipine/benazepril combination therapy for hypertensive patients nonresponsive to benazepril monotherapy. *Am J Hypertens* 2004; **17**:590–596.

8 Yamamoto E, Lai ZF, Yamashita T, Tanaka T, Kataoka K, Tokutomi Y, *et al.* Enhancement of cardiac oxidative stress by tachycardia and its critical role in cardiac hypertrophy and fibrosis. *J Hypertens* 2006; **24**:2057–2069.

9 Jinno T, Iwai M, Li Z, Li JM, Liu HW, Cui TX, *et al.* Calcium channel blocker azelnidipine enhances vascular protective effects of AT1 receptor blocker olmesartan. *Hypertension* 2004; **43**:263–269.

10 Hermsmeyer K, Mishra S, Miyagawa K, Minshall R. Physiologic and pathophysiologic relevance of T-type calcium-ion channels: potential indications for T-type calcium antagonists. *Clin Ther* 1997; **19**:18–26.

11 Ozawa Y, Hayashi K, Nagahama T, Fujiwara K, Saruta T. Effect of T-type selective calcium antagonist on renal microcirculation: studies in the isolated perfused hydronephrotic kidney. *Hypertension* 2001; **38**:343–347.

12 Van der Vring JA, Cleophas TJ, Van der Wall EE, Niemeyer MG. T-channel-selective calcium channel blockade: a promising therapeutic possibility, only preliminarily tested so far: a review of published data. T-Channel Calcium Channel Blocker Study Group. *Am J Ther* 1999; **6**:229–233.

13 Martin RL, Lee JH, Cribbs LL, Perez-Reyes E, Hanck DA. Mibefradil block of cloned T-type calcium channels. *J Pharmacol Exp Ther* 2000; **295**:302–308.

14 Kumar PP, Stotz SC, Paramashivappa R, Beedle AM, Zamponi GW, Rao AS. Synthesis and evaluation of a new class of nifedipine analogs with T-type calcium channel blocking activity. *Mol Pharmacol* 2002; **61**:649–658.

15 Romanin C, Seydl K, Glossmann H, Schindler H. The dihydropyridine niguldipine inhibits T-type Ca2+ currents in atrial myocytes. *Pflugers Arch* 1992; **420**:410–412.

16 Furukawa T, Nukada T, Namiki Y, Miyashita Y, Hatsuno K, Ueno Y, *et al.* Five different profiles of dihydropyridines in blocking T-type Ca(2+) channel subtypes (Ca(v)3.1 (alpha(1G)), Ca(v)3.2 (alpha(1H)), and Ca(v)3.3 (alpha(1I))) expressed in *Xenopus* oocytes. *Eur J Pharmacol* 2009; **613**:100–107.

17 Furukawa T, Nukada T, Miura R, Ooga K, Honda M, Watanabe S, *et al.* Differential blocking action of dihydropyridine Ca2+ antagonists on a T-type Ca2+ channel (alpha1G) expressed in *Xenopus* oocytes. *J Cardiovasc Pharmacol* 2005; **45**:241–246.

18 Sugano N, Wakino S, Kanda T, Tatematsu S, Homma K, Yoshioka K, *et al.* T-type calcium channel blockade as a therapeutic strategy against renal injury in rats with subtotal nephrectomy. *Kidney Int* 2008; **73**:826–834.

19 Horiba M, Muto T, Ueda N, Opthof T, Miwa K, Hojo M, *et al.* T-type Ca2+ channel blockers prevent cardiac cell hypertrophy through an inhibition of calcineurin-NFAT3 activation as well as L-type Ca2+ channel blockers. *Life Sci* 2008; **82**:554–560.

20 Okayama S, Imagawa K, Naya N, Iwama H, Somekawa S, Kawata H, *et al.* Blocking T-type Ca2+ channels with efonidipine decreased plasma aldosterone concentration in healthy volunteers. *Hypertens Res* 2006; **29**:493–497.

21 Takebayashi S, Li Y, Kaku T, Inagaki S, Hashimoto Y, Kimura K, *et al.* Remodeling excitation-contraction coupling of hypertrophied ventricular myocytes is dependent on T-type calcium channels expression. *Biochem Biophys Res Commun* 2006; **345**:766–773.

22 Izumi T, Kihara Y, Sarai N, Yoneda T, Iwanaga Y, Inagaki K, *et al.* Reinduction of T-type calcium channels by endothelin-1 in failing hearts in vivo and in adult rat ventricular myocytes in vitro. *Circulation* 2003; **108**:2530–2535.

23 Cheng XW, Murohara T, Kuzuya M, Izawa H, Sasaki T, Obata K, *et al.* Superoxide-dependent cathepsin activation is associated with hypertensive myocardial remodeling and represents a target for angiotensin II type 1 receptor blocker treatment. *Am J Pathol* 2008; **173**:358–369.

24 Xu J, Nagata K, Obata K, Ichihara S, Izawa H, Noda A, *et al.* Nicorandil promotes myocardial capillary and arteriolar growth in the failing heart of Dahl salt-sensitive hypertensive rats. *Hypertension* 2005; **46**:719–724.

25 Saka M, Obata K, Ichihara S, Cheng XW, Kimata H, Nishizawa T, *et al.* Pitavastatin improves cardiac function and survival in association with suppression of the myocardial endothelin system in a rat model of hypertensive heart failure. *J Cardiovasc Pharmacol* 2006; **47**:770–779.

26 Kass DA, Bronzwaer JG, Paulus WJ. What mechanisms underlie diastolic dysfunction in heart failure? *Circ Res* 2004; **94**:1533–1542.

27 Koitabashi N, Arai M, Kogure S, Niwano K, Watanabe A, Aoki Y, *et al.* Increased connective tissue growth factor relative to brain natriuretic peptide as a determinant of myocardial fibrosis. *Hypertension* 2007; **49**:1120–1127.

28 Mundhenke M, Schwartzkopff B, Strauer BE. Structural analysis of arteriolar and myocardial remodelling in the subendocardial region of patients with hypertensive heart disease and hypertrophic cardiomyopathy. *Virchows Arch* 1997; **431**:265–273.

29 Kelly BD, Hackett SF, Hirota K, Oshima Y, Cai Z, Berg-Dixon S, *et al.* Cell type-specific regulation of angiogenic growth factor gene expression and induction of angiogenesis in nonischemic tissue by a constitutively active form of hypoxia-inducible factor 1. *Circ Res* 2003; **93**:1074–1081.

30 Sano M, Minamino T, Toko H, Miyauchi H, Orimo M, Qin Y, *et al.* p53-induced inhibition of Hif-1 causes cardiac dysfunction during pressure overload. *Nature* 2007; **446**:444–448.

31 Dimmeler S, Fleming I, Fisslthaler B, Hermann C, Busse R, Zeiher AM. Activation of nitric oxide synthase in endothelial cells by Akt-dependent phosphorylation. *Nature* 1999; **399**:601–605.

32 Fulton D, Gratton JP, McCabe TJ, Fontana J, Fujio Y, Walsh K, *et al.* Regulation of endothelium-derived nitric oxide production by the protein kinase Akt. *Nature* 1999; **399**:597–601.

33 Murohara T, Asahara T, Silver M, Bauters C, Masuda H, Kalka C, *et al.* Nitric oxide synthase modulates angiogenesis in response to tissue ischemia. *J Clin Invest* 1998; **101**:2567–2578.

34 Dietz JD, Du S, Bolten CW, Payne MA, Xia C, Blinn JR, *et al.* A number of marketed dihydropyridine calcium channel blockers have mineralocorticoid receptor antagonist activity. *Hypertension* 2008; **51**:742–748.

35 Nagata K, Obata K, Xu J, Ichihara S, Noda A, Kimata H, *et al.* Mineralocorticoid receptor antagonism attenuates cardiac hypertrophy and failure in low-aldosterone hypertensive rats. *Hypertension* 2006; **47**:656–664.

36 Izawa H, Murohara T, Nagata K, Isobe S, Asano H, Amano T, *et al.* Mineralocorticoid receptor antagonism ameliorates left ventricular diastolic dysfunction and myocardial fibrosis in mildly symptomatic patients with idiopathic dilated cardiomyopathy: a pilot study. *Circulation* 2005; **112**:2940–2945.

37 Marcus ML, Koyanagi S, Harrison DG, Doty DB, Hiratzka LF, Eastham CL. Abnormalities in the coronary circulation that occur as a consequence of cardiac hypertrophy. *Am J Med* 1983; **75**:62–66.

38 Tomanek RJ. Response of the coronary vasculature to myocardial hypertrophy. *J Am Coll Cardiol* 1990; **15**:528–533.

39 Shyu KG, Liou JY, Wang BW, Fang WJ, Chang H. Carvedilol prevents cardiac hypertrophy and overexpression of hypoxia-inducible factor-1alpha and vascular endothelial growth factor in pressure-overloaded rat heart. *J Biomed Sci* 2005; **12**:409–420.

40 Giordano FJ, Gerber HP, Williams SP, VanBruggen N, Bunting S, Ruiz-Lozano P, *et al.* A cardiac myocyte vascular endothelial growth factor paracrine pathway is required to maintain cardiac function. *Proc Natl Acad Sci U S A* 2001; **98**:5780–5785.

41 Yoon YS, Uchida S, Masuo O, Cejna M, Park JS, Gwon HC, *et al.* Progressive attenuation of myocardial vascular endothelial growth factor expression is a seminal event in diabetic cardiomyopathy: restoration of microvascular homeostasis and recovery of cardiac function in diabetic cardiomyopathy after replenishment of local vascular endothelial growth factor. *Circulation* 2005; **111**:2073–2085.

42 Matter CM, Mandinov L, Kaufmann PA, Vassalli G, Jiang Z, Hess OM. Effect of NO donors on LV diastolic function in patients with severe pressure-overload hypertrophy. *Circulation* 1999; **99**:2396–2401.

43 Giordano FJ, Ping P, McKirnan MD, Nozaki S, DeMaria AN, Dillmann WH, *et al.* Intracoronary gene transfer of fibroblast growth factor-5 increases blood flow and contractile function in an ischemic region of the heart. *Nat Med* 1996; **2**:534–539.

44 Nayler WG, Yepez CE, Poole-Wilson PA. The effect of beta-adrenoceptor and Ca2+ antagonist drugs on the hypoxia-induced increased in resting tension. *Cardiovasc Res* 1978; **12**:666–674.

45 De Bruyne B, Bronzwaer JG, Heyndrickx GR, Paulus WJ. Comparative effects of ischemia and hypoxemia on left ventricular systolic and diastolic function in humans. *Circulation* 1993; **88**:461–471.

Atherosclerosis 210 (2010) 430–437

Contents lists available at ScienceDirect

Atherosclerosis

journal homepage: www.elsevier.com/locate/atherosclerosis

AT1 blockade attenuates atherosclerotic plaque destabilization accompanied by the suppression of cathepsin S activity in apoE-deficient mice

Takeshi Sasaki[a,b], Masafumi Kuzuya[b,*], Kae Nakamura[b], Xian Wu Cheng[c], Taiju Hayashi[a], Haizhen Song[c], Lina Hu[b], Kenji Okumura[c], Toyoaki Murohara[c], Akihisa Iguchi[b], Kohji Sato[a]

[a] Department of Anatomy and Neuroscience, Hamamatsu University School of Medicine, 1 Handayama, Higashi-ku, Hamamatsu, Shizuoka, Japan
[b] Department of Geriatrics, Nagoya University Graduate School of Medicine, 65 Tsuruma-cho, Showa-ku, Nagoya, Japan
[c] Department of Cardiology, Nagoya University Graduate School of Medicine, 65 Tsurumai-cho, Showa-ku, Nagoya, Japan

ARTICLE INFO

Article history:
Received 25 August 2009
Received in revised form
20 December 2009
Accepted 21 December 2009
Available online 4 January 2010

Keywords:
Angiotensin II type 1 receptor
Olmesartan
Cathepsin S
Plaque vulnerability
Apolipoprotein E deficient mouse
Oxidative stress

ABSTRACT

Although it has been suggested that the renin–angiotensin (RA) system and cathepsins contribute to the development and vulnerability of atherosclerotic plaque, the interaction of the RA system and cathepsins is unclear. Thus, we investigated the effects of an angiotensin II type 1 receptor (AT1) antagonist, olmesartan, on the levels of cathepsins in brachiocephalic atherosclerotic plaque and plaque stabilization in apolipoprotein E (apoE)-deficient mice receiving a high-fat diet.

Under a high fat diet, treatment with olmesartan (3 mg/kg per day) maintained collagen and elastin at high levels and attenuated the plaque development and cathepsin S (Cat S) level in the atherosclerotic plaque of apoE-deficient mice. The administration of olmesartan suppressed the accumulation of macrophages in plaque. Immunoreactivities of Cat S and AT1 were observed in macrophages. The amount of Cat S mRNA and the macrophage-mediated collagenolytic and elastolytic activities in cultured macrophages were increased by exposure to angiotensin II (Ang II), and these effects were diminished by olmesartan and the NADPH-oxidase inhibitor apocynin. These results suggested that Cat S derived from macrophages is involved in the mechanisms of atherosclerotic plaque vulnerability, and AT1 blocker maintained the plaque stabilization alongside the suppression of Cat S and macrophage activities.

1. Introduction

Atherosclerosis is a major contributor to the development of cardiovascular disease, a leading cause of coronary heart disease and central vascular disease in developed countries [1]. It is widely accepted that proteolytic systems have a role in the development of atherosclerosis and plaque vulnerability through the proteolytic degradation of the extracellular matrix (ECM) [2–5]. Cathepsin S (Cat S) and K (Cat K), members of the cysteine protease family, have potent elastolytic and collagenolytic activities [6–9]. The importance of cathepsins in the progression of atherosclerosis and plaque destabilization in concert with extracellular matrix degradation has been suggested. Increased levels of Cat S, Cat K and elastolytic activity have been observed in atherosclerotic plaque [10] and in the neointima following balloon angioplasty [11]. In addition, the pathophysiological importance of Cat S and Cat K in atherosclerosis has been demonstrated using double-knockout mice, Cat S-deficient mice crossbred with LDL receptor-deficient mice [12], or apolipoprotein E (apoE)-deficient mice [13], and Cat K-deficient with apoE-deficient mice [14].

Angiotensin II (Ang II), which is the main effector of the renin–angiotensin (RA) system, plays an important role in vascular homeostasis via two plasma membrane receptors, Ang II receptor type 1 (AT1) and type 2 (AT2) [15]. It is suggested that the RA system contributes not only to hypertension but also to the development and vulnerability of atherosclerotic plaque. In clinical studies, it has been demonstrated that the inhibition of the RA system by either an angiotensin-converting enzyme-inhibitor or an AT1 antagonist reduces cardiovascular disease [16–18]. In experimental studies, Ang II has been shown to accelerate atherogenesis [19], and genetic disruption of the AT1 receptor in apoE-deficient mice has led to the inhibition of atherogenesis [20]. It has been demonstrated that Ang II increases MMP expression and induces the activation of MMP through AT1 in vascular smooth muscle cells [21–23]. Furthermore, the administration of AT1 antagonists resulted in plaque stabilization with the attenuation of MMPs [24–27]; thus, it is suggested that AT1 antagonists have beneficial effects on atherosclerotic progression and plaque stability through the attenuation of MMPs. Although these pleiotropic effects of AT1 antagonists for vascular protection have been noted recently, the effect of AT1 antag-

* Corresponding author. Tel.: +81 52 744 2364; fax: +81 52 744 2371.
E-mail address: kuzuya@med.nagoya-u.ac.jp (M. Kuzuya).

0021-9150/$ – see front matter © 2010 Elsevier Ireland Ltd. All rights reserved.
doi:10.1016/j.atherosclerosis.2009.12.031

onist on another important proteinase, the cathepsins, remains unclear.

In the present study, we focused on the effects of an AT1 antagonist, olmesartan, on plaque stabilization and the levels of cathepsins in brachiocephalic atherosclerotic lesions in apoE-deficient mice on a high fat diet. Here we show that treatment with olmesartan maintained high collagen and elastin levels and attenuated the Cat S level in the atherosclerotic plaque. In addition, olmesartan suppressed the accumulation of macrophages in plaque which expressed Cat S and AT1. These results suggested that Cat S derived from macrophages is involved in the mechanisms of atherosclerotic plaque vulnerability, and AT1 blocker maintained the plaque stabilization through the suppression of Cat S expression and macrophage activities.

2. Materials and methods

2.1. Animals and the experimental protocol

All animal studies were conducted in accordance with the animal care guidelines of Nagoya University Graduate School of Medicine. Male Apoe−/− mice with the C57BL/6 genetic background were bred and maintained in the Laboratory of Animal Experiments at Nagoya University after being originally obtained from Jackson Laboratory. The mice were provided with a standard diet (Oriental Yeast) and tap water ad libitum, and the Apoe−/− mice were started at 8 weeks of age on a Western-type diet (WD) containing 21% fat from lard and 0.15% (wt/wt) cholesterol, and they were maintained on this diet for 8 weeks. Male Apoe−/− mice were used for monocytes isolation from blood at 9 weeks of age.

2.2. Experimental design and measurements of blood pressure (BP) and heart rate (HR)

The Apoe−/− mice were randomly assigned to one of two groups: the control group (0.5% carboxymethylcellulose) and the olmesartan group (donated by Daiichi-Sankyo Pharmaceutical Co., 3 mg/kg per day). The dose of olmesartan was established by reference to a previous report [28]. The treatments were given by oral gavage every day starting the same day that WD was begun.

Systemic BP and HR were determined using a tail-cuff pressure analysis system (Softron BP-98A, Softron) in conscious mice. After 8 weeks of WD, mice underwent trial recordings to warm up, and then three reliable recordings were taken and used for the determination of BP and HR.

2.3. Tissue collection and processing

After measurements of BP and HR, mice were anesthetized by intraperitoneal (ip) pentobarbital injection, and blood samples were collected in heparinized syringes. Mice were perfused through the left cardiac ventricle with isotonic saline and 4% paraformaldehyde in 0.01 mol/L phosphate buffer, pH 7.4, under physiological pressure. The brachiocephalic arteries were removed and immersed in fixative for 16 h (4 °C). For histological and immunohistochemical staining, samples were embedded in paraffin, and 3 μm sections were cut and mounted onto MAS-coated slides (Matsunami).

2.4. Histological and immunohistochemical staining

Paraffin sections were deparaffinized in xylene, rehydrated in decreasing alcohol solutions and stained routinely with hematoxylin and eosin (HE), Elastica van Gieson (EVG) staining for elastin, and picrosirius red (PSR) for collagen. The corresponding sections on separate slides were used for the immunohistochemical staining using goat polyclonal antibodies against Cat S (1:50, Santa Cruz Biotechnology) and Cat K (1:50, Santa Cruz Biotechnology), rabbit polyclonal antibody against α-smooth muscle cell actin (ASMA; 1:100, Neo Marker) and AT1 (1:100, Santa Cruz Biotechnology), and using rat monoclonal antibody against macrophage (Mac 3; 1:40, BD Pharmingen). For Cat S-, Cat K- and AT1-staining, sections were subjected to autoclaving while immersed in Tris–EDTA buffer (pH 9.0) for 1 min at 105 °C before the procedures for antigen retrieval. The sections were preincubated with 5% normal serum and then incubated with primary antibodies for 16 h at 4 °C. The sections were then reacted with alkaline phosphatase (AP)-conjugated secondary antibody against goat, rabbit or mouse IgG (1:200, all from Vector Laboratories) for 2 h at 4 °C. These sections were visualized with an AP substrate kit (Vector Laboratories) according to the manufacturer's instructions. Levamisole (Vector Laboratories) was used as the inhibitor of endogenous AP. The counterstaining for the nucleus was performed with Mayer's hematoxylin or methyl green.

2.5. Plaque morphometry

Collagen and elastin contents were evaluated using the PSR- and EVG-stained positive areas, respectively. Images of sections stained for collagen, elastin, Cat S, Cat K, Mac 3, ASMA and AT1 were analyzed with Scion Image software (Scion Corp.). Three cross-sections of vessels were quantified and averaged per mouse. We set a threshold to automatically compute the positive areas for each stain and then computed the ratio of the positive area to the intimal area.

2.6. Double immunofluorescence

Colocalization studies were performed with double immunofluorescence staining methods. The sections were preincubated with 5% normal serum and incubated with primary antibodies against Cat S, Cat K, Mac 3 and AT1 for 16 h at 4 °C. Immunoreactivity was visualized using Alexa Fluor 488-conjugated anti-rat IgG/Alexa Fluor 594-conjugated anti-goat IgG, or Alexa Fluor 488-conjugated anti-goat IgG/Alexa Fluor 594-conjugated anti-rabbit IgG. All Alexa Fluor-conjugated secondary antibodies (Molecular Probes) were diluted 200-fold for use. Double immunofluoresence of AT1 and ASMA was performed using rabbit polyclonal anti-AT1 antibody and biotinylated mouse monoclonal anti-ASMA antibody (1:100), and this section was visualized using Alexa Fluor 594-conjugated anti-rabbit IgG/fluorescein-conjugated streptavidin (1:50; Vector Laboratories). The slides were mounted in glycerol-based Vectashield medium (Vector Laboratories) containing the nucleus stain 4′,6-diamidino-2-phenylindole (DAPI).

2.7. Cell isolation and culture and stimulation

Monocytes (MNCs) were isolated from Apoe−/− mice (9 weeks of age) peripheral blood by Histopaque solution (Histopaque 1083, Sigma–Aldrich). The collected cell was washed 3 times with phosphate-buffered saline and re-suspended at 1.5×10^6 cells/mL in a conditioned medium consisting of RPMI 1640 (GIBCO) medium supplemented with 2 mmol/L glutamine, 10% heat-inactivated (56 °C, 30 min) fetal bovine serum (FBS), and antibiotics. Cells were seeded in 24-well plates at 2 mL/well (Iwaki Glass) and allowed to adhere to tissue culture plates for 2 h at 37 °C before gentle rinsing to remove nonadherent cells. Following differentiation to macrophages which was confirmed by expression of CD68 (Chemicon International, Inc., Temecula, CA) by immunofluorescence, differentiation to foam cells was induced by addition of acetylated low-density lipoprotein (80 μg/mL, Harbor Bio-Products,

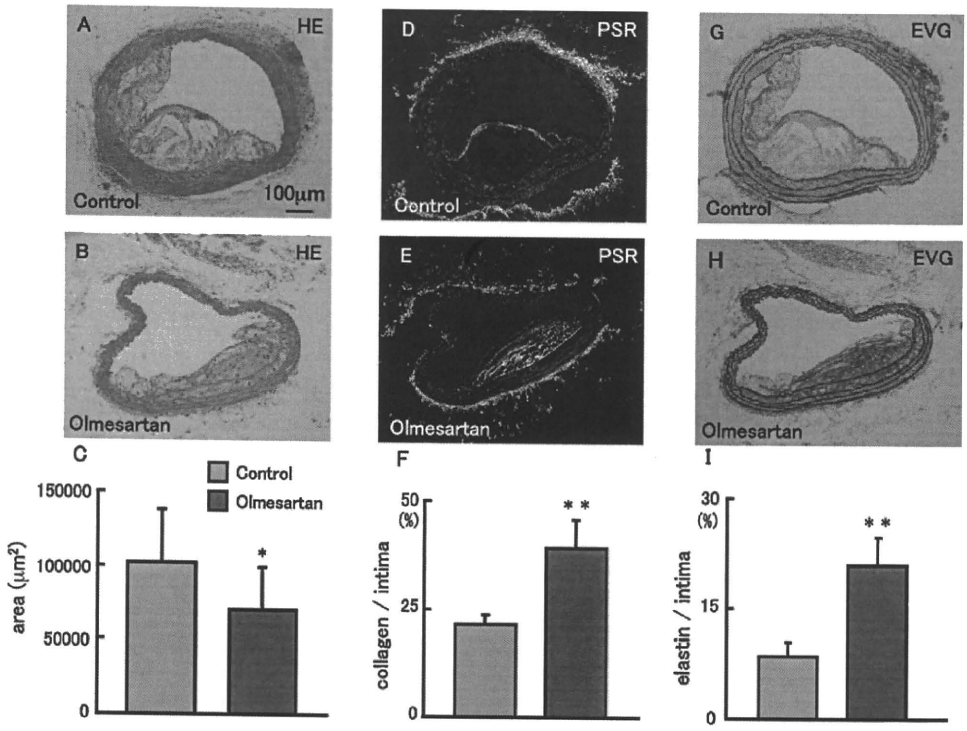

Fig. 1. The effect of olmesartan on atherosclerotic plaque progression (A–C) and intimal levels of collagen (D–F) and elastin (G–I) in the brachiocephalic artery of apoE-deficient mice. ApoE-deficient mice were given a high-cholesterol diet for 8 weeks, and cross-sections of the brachiocephalic artery were prepared. Collagen was stained by PSR and visualized by polarized microscopy. Elastin contents were evaluated using the EVG-stained positive area. Olmesartan administration significantly decreased atherosclerotic lesion formation and maintained high levels of collagen and elastin. Values are means ± SD, $n = 8$. $^{*}P < 0.05$, $^{**}P < 0.01$ versus control.

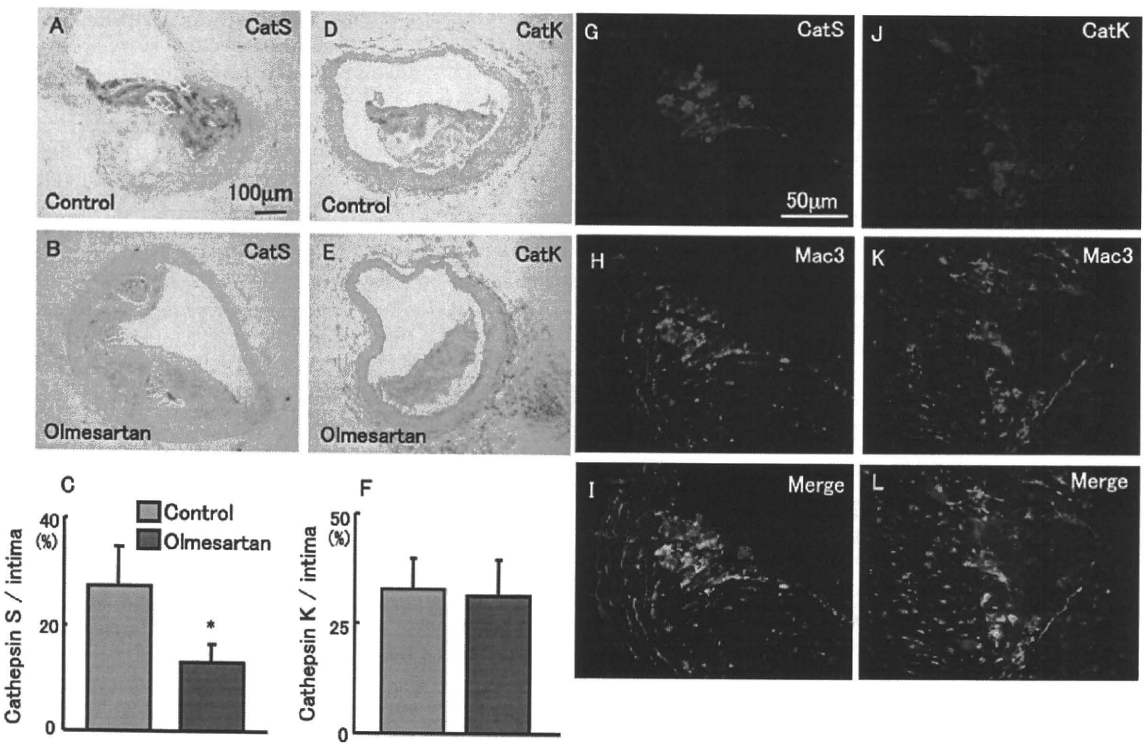

Fig. 2. Effect of olmesartan on the expression of Cat S (A–C) and Cat K (D–F) in the brachiocephalic artery of apoE-deficient mice. Olmesartan administration significantly attenuated the Cat S immunostaining but not that of Cat K. Values are means ± SD, $n = 8$. $^{*}P < 0.01$ versus control. Double staining of macrophage (Mac 3) and Cat S (D–I) or Cat K (J–L) in the brachiocephalic artery of apoE-deficient control mice. Colocalization of Cat S and Mac 3 was observed in the shoulder region (I), a vulnerable site of atherosclerotic plaque. Cat K colocalized with Mac 3 in atherosclerotic plaque (L).

Norwood, MA) for 48 h, and were cultured serum-free RPMI 1640 for overnight for using cell stimulation assays.

2.8. Real-time reverse transcription-polymerase chain reaction

Total RNA was extracted from cell extracts using a Qiagen RNeasy Micro Kit (Qiagen Inc.) following the manufacturer's instructions, and the abundance of specific mRNAs was determined by reverse-transcription (RT) and real-time quantitative polymerase chain reaction (PCR) analysis as described previously [11]. The sequences of the primers and probes for mouse Cat S are (forward) 5′-GTGGCCACTAAAGGGCCTG-3′, (reverse) 5′-ACCGCTTTTGTAGAAGAAGAAGGAG-3′, and (probe) 5′-TCTGTGGGCATCGACGCCAGC-3′; and Cat K are (forward) 5′-AGCAGGCTGGAGGACTAAGGT-3′, (reverse) 5′-TTTGTGCATCTCAGTGGAAGACT-3′, and (probe) 5′-ACCTTCCCGAGCCCCTGTCTTCGTA-3′; glyceraldehyde 3-phosphate dehydrogenase (GAPDH) was measured in parallel with genes of interest and used as an internal standard.

2.9. Elastase and collagenase assays

Differentiation of macrophage to foam cells were cultured in 24-well plates until confluent. After overnight starvation in FBS free Hanks's balanced salt solution (GIBCO), the cells were pretreatment with or without apocynin (100 μmol/L, Sigma–Aldrich), or olmesartan (1 μmol/L), and then were cultured in the presence or absence of Ang II (0.1 μmol/L, Sigma–Aldrich) in serum-free medium containing either BODIPY® fluorescein-conjugated DQTM elastin from bovine neck ligament (300 μg/well, Molecular Probes, Eugene, OR) or water-insoluble nondenatured fluorescein-labeled collagen-type I (300 μg/well, Calbiochem, Darmstadt, Germany). After 24 h of incubation, culture media were analyzed for degraded elastin or collagen by Fluoroskan Ascent CF (Labsystems, Helsinki, Finland; excitation/emission: 485/530) [29]. To evaluate the role of Cat S, the reactions were also performed in presence or absence of a specific inhibitor of Cat S, morpholinerea-leucine-homophenylalanine-vinylsulfone-phenyl (LHVS, 5 μmol/L). Data were presented as relative units after adjustment for background levels. Data were representative of at least four independent experiments.

2.10. Statistical analysis

Data were shown as means ± SD. Differences were analyzed by Student's *t*-test or by one-way analysis of variance with the *F*-test followed by Scheffe's multiple comparison test. A *P*-value of <0.05 was considered statistically significant.

3. Results

3.1. The effect of olmesartan on plaque morphology and cathepsins expression in brachiocephalic artery of apoE-deficient mice

Olmesartan at 3 mg/kg per day did not significantly affect arterial BP, HR, or body weight (control and olmesartan-treated apoE-deficient mice, mean arterial BP: 77.3 ± 5.4 mmHg and 73.0 ± 5.4 mmHg, HR: 597.4 ± 41.2 bpm and 616.5 ± 32.4 bpm, body weight: 25.8 ± 4.5 g and 26.1 ± 4.5 g, respectively; mean ± SD, $n = 8$). Olmesartan administration significantly decreased atherosclerotic lesion formation in the brachinocephalic artery of apoE-deficient mice after 8 weeks WD diet supplementation ($P < 0.05$; Fig. 1A–C). In the histological analysis of the collagen by PSR-staining visualized with polarized light, significantly higher collagen content was observed in olmesartan-treated mice compared with controls ($P < 0.01$; Fig. 1D–F). In addition, the elastin levels determined by EVG-staining remained significantly higher in olmesartan-treated mice compared with control mice ($P < 0.01$; Fig. 1G–I). Although the intense immunoreactivity of Cat S was observed in atherosclerotic lesions in the brachinocephalic artery in control mice, mainly in atheromatous plaque and in peripheral fibrous cap with weaker immunoreactivity than atheromatous plaque, the treatment with olmesartan significantly attenuated the Cat S immunostaining ($P < 0.01$; Fig. 2A–C), whereas olmesartan administration did not affect the expression of Cat K (Fig. 2D–F). Double immunofluorescence staining in the brachiocephalic artery of apoE-deficient control mice demonstrated that Cat S colocalized with the macrophage marker Mac 3 in the shoulder region of the plaque, a vulnerable site of atherosclerotic plaque (Fig. 2G–I). In addition, colocalization of Cat K and Mac 3 was also detected in atherosclerotic plaque (Fig. 2J–L).

3.2. The effect of olmesartan on macrophage and smooth muscle cell accumulation in brachiocephalic atherosclerotic legion of apoE-deficient mice

Extensive immunostaining of Mac 3 for macrophages in the intima of atherosclerotic plaque was detected in control apoE-deficient mice, while this Mac 3-positive area was significantly diminished by olmesartan administration ($P < 0.05$, Fig. 3A–C). The immunoreactivity of ASMA was mainly observed in the media and intimal fibrous cap of atherosclerotic lesions (Fig. 3D). No significant difference in the intimal ASMA-positive area was observed between olmesartan-treated mice and control mice (Fig. 3E and F).

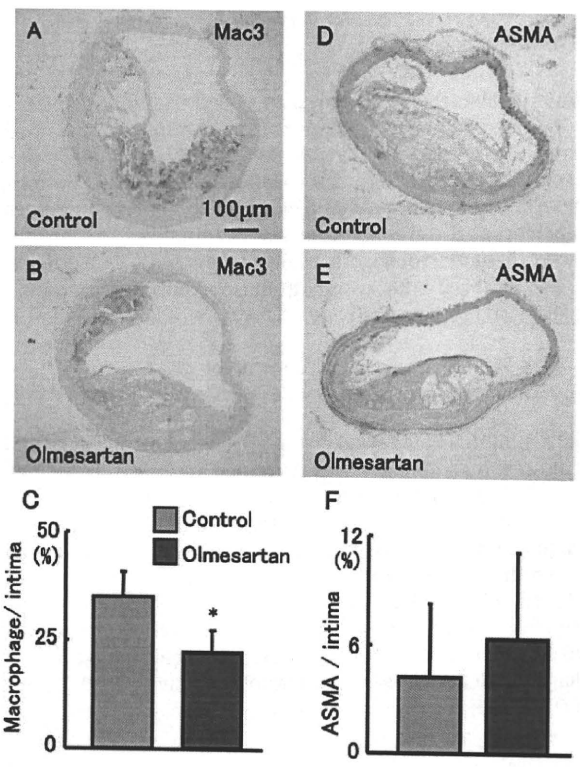

Fig. 3. Effect of olmesartan on macrophage (A–C) and smooth muscle cell accumulation (D–F) in the brachiocephalic artery of apoE-deficient control mice. Olmesartan administration significantly diminished the immunostaining area of Mac 3, but did not significantly affect the immunostaining area of ASMA. Values are means ± SD, $n = 8$. *$P < 0.05$ versus control.

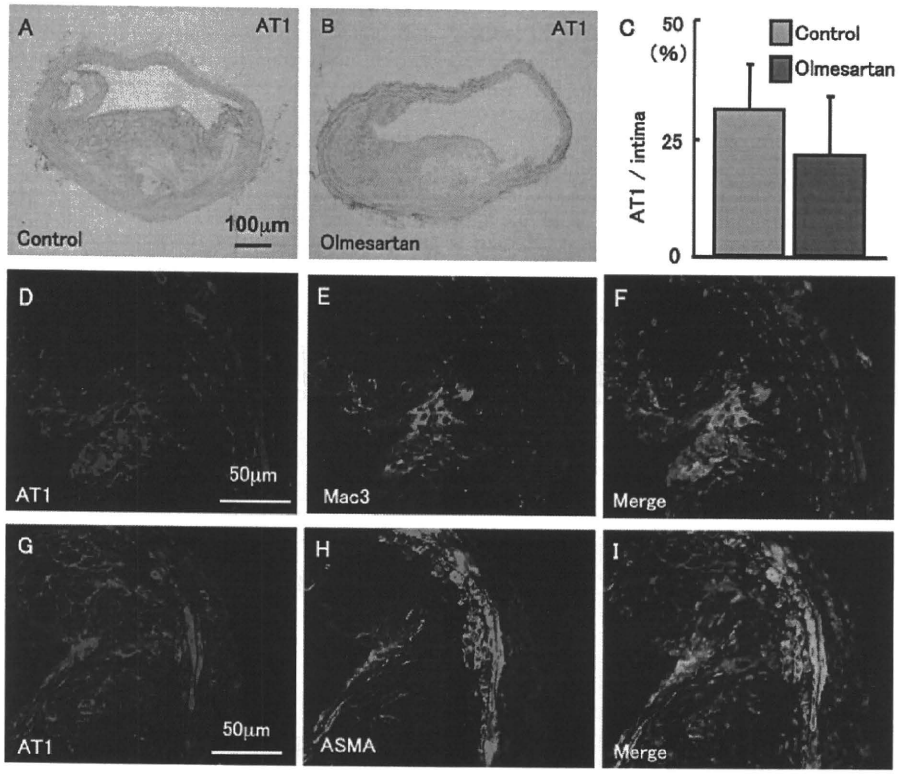

Fig. 4. Effect of olmesartan on the expression of AT1 receptor (A–C) in the brachiocephalic artery of apoE-deficient mice. Strong immunoreactivity of the AT1 receptor was observed in foam cells. Treatment with olmesartan did not significantly change the immunostaining of AT1 receptor. Values are means ± SD, $n = 8$. Double staining of AT1 receptor and macrophage (Mac 3; D–I) or smooth muscle cell actin (ASMA; J–L) in the brachiocephalic artery of apoE-deficient control mice. Colocalization of AT1 receptor and Mac 3 was detected in intimal lesions (I). Colocalization of AT1 receptor and ASMA was mainly observed in the fibrous cap and media (L).

3.3. Expression of AT1 receptor in brachiocephalic artery of apoE-deficient mice

Immunohistochemical analysis revealed that wide and intense AT1 immunostaining was observed at the intimal and medial regions (Fig. 4A and B). There is no significant difference in the AT1-positive area in atheromatous lesions between the control and olmesartan-treated groups (Fig. 4C). Double immunofluorescence of brachiocephalic artery sections with antibodies to the smooth muscle cell- or macrophage-specific markers and AT1 revealed that AT1 was localized both in smooth muscle cells and macrophages (Fig. 4D–F and H–J, respectively).

3.4. Regulation of Cat S and Cat K expression and activity in cultured macrophages

Real-time RT-PCR revealed that the amount of Cat S mRNA in cultured macrophages was increased by exposure to Ang II ($P < 0.01$), and this effect was inhibited again by olmesartan and apocynin, a NADPH-oxidase inhibitor ($P < 0.01$; Fig. 5A), whereas, no significant difference of Cat K mRNA was observed among these groups (Fig. 5B). Furthermore, Ang II enhanced macrophage-mediated collagenolytic and elastolytic activities ($P < 0.01$), and these effects were inhibited by the administration of olmesartan ($P < 0.01$), apocynin ($P < 0.01$), and LHVS, a specific inhibitor of Cat S (collagenolytic activity: $P < 0.05$, elastolytic activity: $P < 0.01$; Fig. 5C and D).

4. Discussion

In this study, we demonstrated that treatment with AT1 antagonist olmesartan resulted in stabilization of atherosclerotic plaque by higher levels of elastin and collagen in the plaque. Concomitantly, the expression of Cat S that is elastolytic and collagenolytic protease was suppressed in the intima by treatment with olmesartan. In addition, an in vitro experiment indicated that the expression of Cat S and elastolytic or collagenolytic activity induced by Ang II in cultured macrophages was attenuated by the administration of olmesartan. Furthermore, the accumulation of macrophages was inhibited by olmesartan administration. The colocalization of macrophages and Cat S was observed in atherosclerotic plaque. Taken together, our data suggest that Cat S derived from macrophages is involved in the mechanisms of atherosclerotic plaque vulnerability via ECM degradation, and that AT1 blocker maintained plaque stabilization through the suppression of both macrophage accumulation and the Cat S expression of macrophages.

In advanced atherosclerotic lesions, Ang II stimulates expression of MMPs [30–32], leading to destabilization of atherosclerotic plaque. Moreover, a previous report suggested that an AT1 receptor antagonist, irbesartan, contributes to plaque stabilization by the inhibition of MMPs in humans [24]. We also confirmed the high immunoreactivities of MMP-8 and MMP-9 in atherosclerotic lesions of WD-fed apoE-deficient mice, and the administration of olmesartan attenuated the expression of both MMP-8 and MMP-9 (data not shown). Moreover, these MMPs colocalized with the macrophage marker Mac 3 (data not shown). Therefore, the suppression of not only Cat S but also MMPs by olmesartan administration contributes to the maintenance of high levels of collagen and elastin in atherosclerotic plaque and helps to stabilize the plaque in apoE-deficient mice.

The treatment with olmesartan resulted in stable plaque in apoE-deficient mice in this study. Olmesartan administration was simultaneously commenced with WD feeding, therefore, it is sug-

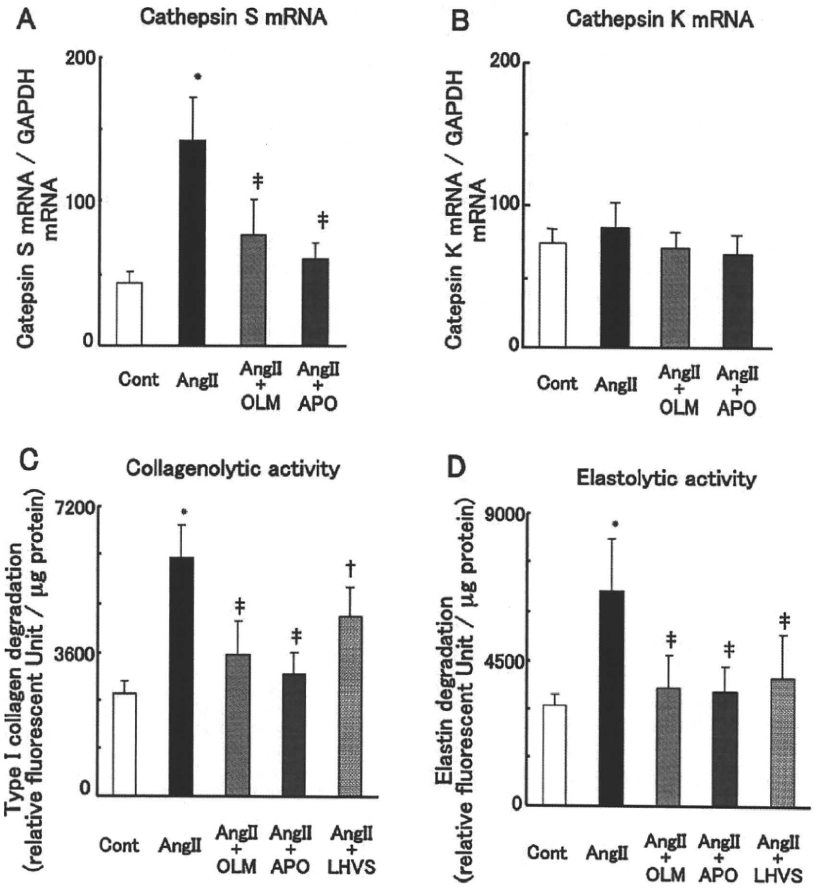

Fig. 5. Regulation of Cat S (A) and Cat K (B) expression and collagenolytic (C) and elastolytic (D) activity in cultured macrophages. Following pretreatment with olmesartan (OLM; 1 μmol/L), apocynin (APO; 100 μmol/L) and morpholinerea-leucine-homophenylalanine-vinylsulfone-phenyl (LHVS; 5 μmol/L), respectively, for 30 min, the cells were cultured in the presence or absence of angiotensin II (Ang II; 0.1 μmol/L) for 24 h. They were then subjected to quantitative real-time PCR analysis of Cat S (A) and Cat K (B) mRNA or to assay of collagenolytic activity (C) and elastolytic activity (D). Quantitative data are means ± SD ($n = 6$). $^{*}P < 0.01$ versus corresponding controls; $^{\ddagger}P < 0.05$, $^{\dagger}P < 0.01$ versus cells treated with Ang II alone.

gested that olmesartan might affect not only the matrix proteolysis in atherosclerotic plaque but also the plaque composition which was configured and altered at initiation and early-stage of plaque formation. Further investigations will be required to clarify these issues.

The mechanisms of olmesartan-induced Cat S suppression still remain unclear. Recently, Cheng et al. reported that AT1 receptor is involved in the activation of Cat S depending on the superoxide production during hypertensive myocardial remodeling [33]. It is well-known that the RA system contributes to superoxide production through NADPH-oxidase [28,34]; therefore, olmesartan may suppress Cat S levels via AT1 receptor-mediated superoxide production systems. Indeed, the expression of Cat S and the activity of extracellular matrix catabolism induced by Ang II in cultured macrophages were attenuated by the administration of apocynin, a NADPH-oxidase inhibitor. Furthermore, we observed the colocalization of the immunoreactivities of AT1 receptor and N(epsilon)-(hexanoyl)lysine (unpublished data), which is an oxidative stress biomarker [35,36]. On the other hand, daily administration of olmesartan did not affect BP, but maintained the high contents of collagen and elastin in atherosclerotic plaque, which were indices of plaque stabilization, in apoE-deficient mice in this study. This result supported the hypothesis that atherosclerotic plaque was stabilized not through BP suppression but through another pleiotropic effect of olmesartan. In our mouse model, we still have not determined whether the effect of olmesartan on plaque stabilization is only mediated by the attenuation of free-radical-induced Cat S expression in macrophages. Further investigations will be required. Treatment of olmesartan had no effect on Cat K expression in atherosclerotic plaque. In cultured macrophages experiment, administration of olmesartan did not affect the levels of Cat K mRNA. From these results, it is suggested that AT1 receptor may not be involved in regulation of Cat K expression.

Previous reports revealed the expression of Cat S and Cat K in macrophages and smooth muscle cells in atherosclerotic plaque [10,12,37]. In the present study we also found that the strong expression of Cat S and AT1 was observed in intimal lesions. Immunofluorescent studies also showed the expression of AT1 on macrophages. Furthermore, the expression of Cat S and elastase activity in cultured macrophages was stimulated by treatment with Ang II. The elastolytic and collagenolytic activity induced by Ang II was inhibited by LHVS, a specific inhibitor of Cat S, suggesting a possible role for Cat S in Ang II-induced proteolysis of ECMs. Therefore, Cat S released from macrophages may participate in the mechanisms of atherosclerotic plaque vulnerability via catabolization of the ECMs including elastin and collagen. However, since the expression of Cat S and Cat K was detected in the fibrous cap of atherosclerotic plaque in our experiment, it is possible that Cat S and Cat K derived from smooth muscle cells may also be involved in the progression of atherosclerotic plaque vulnerability.

The immunoreactive Mac 3-positive area that was thought to be macrophage accumulation was significantly reduced in brachiocephalic atherosclerotic plaque of apoE-deficient mice by means of olmesartan administration. It has been reported that the AT1 antagonist irbesartan strongly decreased the levels of monocyte chemoattractant protein-1 mRNA and immunostaining in the lesion area, which are involved in macrophage infiltration into the lesion area [38]. In addition, Ang II upregulates the expression of adhesion molecules [39,40] thought to participate in monocyte accumulation in the vessel wall and to contribute to the development of atherosclerotic lesions. Therefore, olmesartan might suppress the accumulation of macrophages in plaque through the moderation of several chemokines and adhesion molecules as well as another AT1 antagonist.

Finally, the RA system and ECM proteases including cathepsins and MMPs may be greatly involved in the mechanisms of atherosclerotic plaque vulnerability, and inhibition of the RA system and these proteases by the AT1 antagonist might be beneficial in a treatment strategy for atherosclerosis and may stabilize plaques.

4.1. Perspectives

Our results demonstrated that treatment with olmesartan resulted in stabilization of atherosclerotic plaque alongside the suppression of Cat S and macrophage activities. Our findings support that an interventional treatment with olmesartan is expected to contribute to the inhibition of cardiovascular events. In future investigations, it will be of interest to elucidate the molecular mechanisms of the suppression of Cat S and macrophage activity by olmesartan.

Acknowledgement

Sources of Funding: This work was supported by research grants from the Scientific Research Fund of the Ministry of Education, Science, and Cultures, Japan (No. 19700366).

Disclosures: None.

References

[1] Katagiri H, Yamada T, Oka Y. Adiposity and cardiovascular disorders: disturbance of the regulatory system consisting of humoral and neuronal signals. Circ Res 2007;101:27–39.
[2] Kuzuya M, Iguchi A. Role of matrix metalloproteinases in vascular remodeling. J Atheroscler Thromb 2003;10:275–82.
[3] Liu J, Sukhova GK, Sun JS, et al. Lysosomal cysteine proteases in atherosclerosis. Arterioscler Thromb Vasc Biol 2004;24:1359–66.
[4] Garcia-Touchard A, Henry TD, Sangiorgi G, et al. Extracellular proteases in atherosclerosis and restenosis. Arterioscler Thromb Vasc Biol 2005;25:1119–27.
[5] Lutgens SP, Cleutjens KB, Daemen MJ, Heeneman S. Cathepsin cysteine proteases in cardiovascular disease. FASEB J 2007;21:3029–41.
[6] Shi GP, Munger JS, Meara JP, Rich DH, Chapman HA. Molecular cloning and expression of human alveolar macrophage cathepsin S, an elastinolytic cysteine protease. J Biol Chem 1992;267:7258–62.
[7] Maciewicz RA, Etherington DJ. A comparison of four cathepsins (B, L, N and S) with collagenolytic activity from rabbit spleen. Biochem J 1998;256:433–40.
[8] Cheng XW, Obata K, Kuzuya M, et al. Elastolytic cathepsin induction/activation system exists in myocardium and is upregulated in hypertensive heart failure. Hypertension 2006;48:979–87.
[9] Cheng XW, Kuzuya M, Nakamura K, et al. Localization of cysteine protease, cathepsin S, to the surface of vascular smooth muscle cells by association with integrin alphanubeta3. Am J Pathol 2006;168:685–94.
[10] Sukhova GK, Shi G-P, Simon DI, Chapman HA, Libby P. Expression of the elastolytic cathepsins S and K in human atheroma and regulation of their production in smooth muscle cells. J Clin Invest 1998;102:576–83.
[11] Cheng XW, Kuzuya M, Sasaki T, et al. Increased expression of elastolytic cysteine proteases, cathepsins S and K, in the neointima of balloon-injured rat carotid arteries. Am J Pathol 2004;164:243–51.
[12] Sukhova GK, Zhang Y, Pan JH, et al. Deficiency of cathepsin S reduces atherosclerosis in LDL receptor-deficient mice. J Clin Invest 2003;111:897–906.
[13] Rodgers KJ, Watkins DJ, Miller AL, et al. Destabilizing role of cathepsin S in murine atherosclerotic plaques. Arterioscler Thromb Vasc Biol 2006;26:851–6.
[14] Lutgens E, Lutgens SP, Faber BC, et al. Disruption of the cathepsin K gene reduces atherosclerosis progression and induces plaque fibrosis but accelerates macrophage foam cell formation. Circulation 2006;113:98–107.
[15] Vaughan DE. AT1 receptor blockade and atherosclerosis: hopeful insights into vascular protection. Circulation 2000;101:1496–7.
[16] The Heart Outcomes Prevention Evaluation Study Investigators. Effects of an angiotensin-converting enzyme inhibitor, ramipril, on death from cardiovascular causes, myocardial infarction, and stroke in high-risk patients. N Engl J Med 2000;342:145–53.
[17] The European Trial on Reduction of Cardiac Events with Perindopril in Stable Coronary Artery Disease Investigators. Efficacy of perindopril in reduction of cardiovascular events among patients with stable coronary artery disease: randomised, double-blind, placebo-controlled, multicentre trial (EUROPA). Lancet 2003;362:782–8.
[18] Fliser D, Buchholz K, Haller H. European Trial on Olmesartan and Pravastatin in Inflammation and Atherosclerosis (EUTOPIA) Investigators. 1. Antiinflammatory effects of angiotensin II subtype 1 receptor blockade in hypertensive patients with microinflammation. Circulation 2004;110:1103–7.
[19] Weiss D, Kools JJ, Taylor WR. Angiotensin II-induced hypertension accelerates the development of atherosclerosis in apoE-deficient mice. Circulation 2001;103:448–54.
[20] Wassmann S, Czech T, van Eickels M, et al. Inhibition of diet-induced atherosclerosis and endothelial dysfunction in apolipoprotein E/angiotensin II type 1A receptor double-knockout mice. Circulation 2004;110:3062–7.
[21] Browatzki M, Larsen D, Pfeiffer CA, et al. Angiotensin II stimulates matrix metalloproteinase secretion in human vascular smooth muscle cells via nuclear factor-kappaB and activator protein 1 in a redox-sensitive manner. J Vasc Res 2005;42:415–23.
[22] Wang M, Zhang J, Spinetti G, et al. Angiotensin II activates matrix metalloproteinase type II and mimics age-associated carotid arterial remodeling in young rats. Am J Pathol 2005;167:1429–42.
[23] Guo RW, Yang LX, Wang H, Liu B, Wang L. Angiotensin II induces matrix metalloproteinase-9 expression via a nuclear factor-kappaB-dependent pathway in vascular smooth muscle cells. Regul Pept 2008;147:37–44.
[24] Cipollone F, Fazia M, Iezzi A, et al. Blockade of the angiotensin II type 1 receptor stabilizes atherosclerotic plaques in humans by inhibiting prostaglandin E2-dependent matrix metalloproteinase activity. Circulation 2004;109:1482–8.
[25] Liang C, Wu ZG, Ding J, et al. Losartan inhibited expression of matrix metalloproteinases in rat atherosclerotic lesions and angiotensin II-stimulated macrophages. Acta Pharmacol Sin 2004;25:1426–32.
[26] Suganuma E, Babaev VR, Motojima M, et al. Angiotensin inhibition decreases progression of advanced atherosclerosis and stabilizes established atherosclerotic plaques. J Am Soc Nephrol 2007;18:2311–9.
[27] Fukuda D, Sata M, Ishizaka N, Nagai R. Critical role of bone marrow angiotensin II type 1 receptor in the pathogenesis of atherosclerosis in apolipoprotein E deficient mice. Arterioscler Thromb Vasc Biol 2008;28:90–6.
[28] Tsuda M, Iwai M, Li JM, et al. Inhibitory effects of AT1 receptor blocker, olmesartan, and estrogen on atherosclerosis via anti-oxidative stress. Hypertension 2005;45:545–51.
[29] Liu J, Sukhova GK, Yang JT, et al. Cathepsin L expression and regulation in human abdominal aortic aneurysm, atherosclerosis, and vascular cells. Atherosclerosis 2006;184:302–11.
[30] Galis ZS, Khatri JJ. Matrix metalloproteinases in vascular remodeling and atherogenesis: the good, the bad, and the ugly. Circ Res 2002;90:251–62.
[31] Chen J, Li D, Schaefer RF, Mehta JL. Inhibitory effect of candesartan and rosuvastatin on cd40 and mmps expression in apo-e knockout mice: novel insights into the role of ras and dyslipidemia in atherogenesis. J Cardiovasc Pharmacol 2004;44:446–52.
[32] Luchtefeld M, Grote K, Grothusen C, et al. Angiotensin II induces mmp-2 in a p47phox-dependent manner. Biochem Biophys Res Commun 2005;328:183–8.
[33] Cheng XW, Murohara T, Kuzuya M, et al. Superoxide-dependent cathepsin activation is associated with hypertensive myocardial remodeling and represents a target for angiotensin II type 1 receptor blocker treatment. Am J Pathol 2008;173:358–69.
[34] Rueckschloss U, Quinn MT, Holtz J, Morawietz H. Dose-dependent regulation of NAD(P)H oxidase expression by angiotensin II in human endothelial cells: protective effect of angiotensin II type 1 receptor blockade in patients with coronary artery disease. Arterioscler Thromb Vasc Biol 2002;22:1845–51.
[35] Kato Y, Mori Y, Makino Y, et al. Formation of N&supε;-(hexanonyl)lysine in protein exposed to lipid hydroperoxide. A plausible marker for lipid hydroperoxide-derived protein modification. J Biol Chem 1999;274:20406–14.
[36] Fukuchi Y, Miura Y, Nabeno Y, et al. Immunohistochemical detection of oxidative stress biomarkers, dityrosine and N(epsilon)-(hexanoyl)lysine, and C-reactive protein in rabbit atherosclerotic lesions. J Atheroscler Thromb 2008;15:185–92.
[37] Samokhin AO, Wong A, Saftig P, Brömme D. Role of cathepsin K in structural changes in brachiocephalic artery during progression of atherosclerosis in apoE-deficient mice. Atherosclerosis 2008;200:58–68.
[38] Dol F, Martin G, Staels B, et al. Angiotensin AT1 receptor antagonist irbesartan decreases lesion size, chemokine expression, and macrophage accumulation in apolipoprotein E-deficient mice. J Cardiovasc Pharmacol 2001;38:395–405.